# On salt stress, PLETHORA signaling maintains root meristems

Developmental Cell

Hao, Rong; Zhou, Wenkun; Li, Jingrui; Luo, Manqing; Scheres, Ben et al

https://doi.org/10.1016/j.devcel.2023.06.012

Article

Developmental Cell

# On salt stress, PLETHORA signaling maintains root meristems

## Graphical abstract

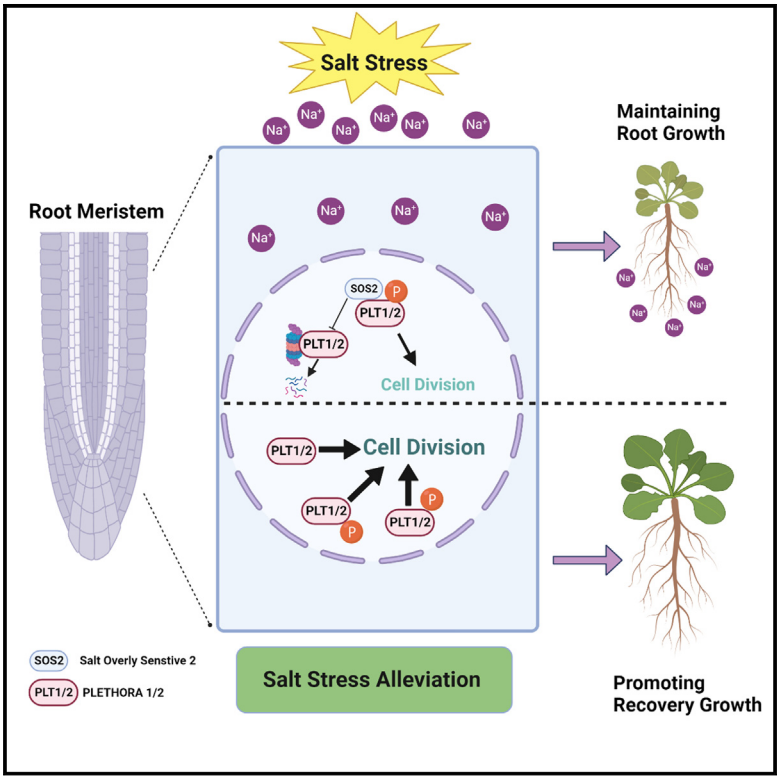


## Highlights

- Root meristem maintenance is critical for plant salt stress tolerance
- SOS2 phosphorylates and stabilizes PLT1/2 proteins under salt stress
- Phosphorylated PLT modulates cell division to maintain root growth under salt stress
- PLT1/2 promotes recovery growth from salt alleviation

## Authors

Rong Hao, Wenkun Zhou, Jingrui Li, Manqing Luo, Ben Scheres, Yan Guo

## Correspondence

zhouwenkun@cau.edu.cn (W.Z.), guoyan@cau.edu.cn (Y.G.)

## In brief

Hao et al. report that salt signaling in *Arabidopsis* activates SOS2 to stabilize PLT1/2 proteins via phosphorylation, and phosphorylated PLT1/2 maintains meristem activity under both salt stress and recovery of root growth after stress alleviation.

Hao et al., 2023, Developmental Cell *58*, 1657–1669
September 25, 2023 
https://doi.org/10.1016/j.devcel.2023.06.012

CellPress

Developmental Cell

CellPress

Article

# On salt stress, PLETHORA signaling maintains root meristems

Rong Hao,[1] Wenkun Zhou,[1,*] Jingrui Li,[1] Manqing Luo,[1] Ben Scheres,[2,3] and Yan Guo[1,4,*]

[1]State Key Laboratory of Plant Environmental Resilience, College of Biological Sciences, China Agricultural University, Beijing 100193, China

[2]Laboratory of Plant Developmental Biology, Wageningen University and Research, 6708 PB Wageningen, the Netherlands

[3]Rijk Zwaan R&D, 4793 RS Fijnaart, the Netherlands

[4]Lead contact

*Correspondence: zhouwenkun@cau.edu.cn (W.Z.), guoyan@cau.edu.cn (Y.G.)

https://doi.org/10.1016/j.devcel.2023.06.012

## SUMMARY

Salt stress is one of the unfavorable environmental factors to affect plants. Salinity represses root growth, resulting in reduced biomass of agricultural plants. Little is known about how plants maintain root growth to counteract salt stress. The AP2-domain transcription factors PLETHORA1/2 (PLT1/2) act as master regulators in root meristem maintenance in *Arabidopsis*. In this study, we report that the salt overly sensitive (SOS) pathway component SOS2 regulates PLT1/2 at the post-transcriptional level. Salt-activated SOS2 interacts and phosphorylates PLT1/2 through their conserved C-terminal motifs to stabilize PLT1/2, critical for root apical meristem maintenance under salt stress. The phospho-mimetic version of PLT1/2 restored meristem and primary root length reduction of *sos2-2* and *plt1-4 plt2-2* mutants on salt treatment. Moreover, SOS2-mediated PLT1/2 phosphorylation improves root growth recovery after salt stress alleviation. We identify a SOS2-PLT1/2 core protein module that is required for protecting primary root growth and meristem maintenance from salt stress.

## INTRODUCTION

Salt stress is a major environmental stress that restricts crop yield and threatens food security.[1–3] Salt stress, commonly caused by high concentrations of sodium ($Na^+$) and chloride ions, induces osmotic stress, ionic stress, and secondary stress.[2,4] Salt stress represses whole plant growth, and especially root growth. In the root meristem, cell division is rapidly inhibited in response to salt, leading to reduced primary root growth.[5] Salt stress also alters root system architecture by regulating root gravity, lateral root initiation, and elongation.[6–9] Root meristem maintenance under salt stress contributes to salt-tolerated adaptive root growth. However, the molecular mechanism of salt-mediated meristem maintenance has remained elusive.

Over the years, numerous studies in *Arabidopsis* have revealed key components involved in the salt stress signaling.[1] Among them, the salt overly sensitive (SOS) pathway is best characterized, in mediating ion homeostasis through $Na^+$ efflux from the cytosol to the outside of cells.[10–15] Salt stress rapidly increases the cytosolic $Ca^{2+}$ concentration within seconds,[16] and $Ca^{2+}$ binds and activates the SOS3/SCaBP8 myristoylated calcium-binding proteins.[17–19] SOS3/SCaBP8 interact with the core component SOS2 and recruit it to the plasma membrane to phosphorylate $Na^+/H^+$ antiporter SOS1 and to exclude $Na^+$ and reduce $Na^+$ in cytoplast.[10,12,14] Previous studies reported that SOS3 regulates lateral root growth and rearranges the auxin gradient,[20] but the molecular mechanism of the SOS pathway in regulating primary root growth under salt stress has not been elucidated.

Primary root growth is maintained by repeated divisions of cells in the meristem and continuous divisions in stem cells.[21,22] The GRAS (acronym of GIBBERELLIN INSENSITIVE [GAI], REPRESSOR OF GA1–3 [RGA], and SCARECROW [SCR] genes) family transcription factors SHORT-ROOT (SHR) and SCR, together with transcriptional cofactors, provide positional information in the radial axis to regulate quiescent center (QC) specification, asymmetric division of cortex/endodermal stem cells, and maintenance of the meristem.[23–29] In parallel to the SHR/SCR pathway, the APETALA2 (AP2)-domain transcription factor PLETHORAs (PLTs) displays a gradient distribution in the longitudinal axis of the meristem, with a maximum around the root stem cell niche (SCN).[30–32] The phytohormone auxin induces *PLTs* expression, and in turn, PLTs stabilize auxin to the maximum by regulating *PINFORMED* (*PIN*) expression.[33] Previous studies reported that the root growth factor (RGF) peptides regulate *PLTs* at transcriptional and post-transcriptional levels.[34–37] However, little is known about the regulation of PLT proteins under stress conditions.

Here, we show that the PLT pathway is required for maintenance of meristem activity under salt stress. SOS2 modulates PLT1 and PLT2 expression at post-transcriptional level via phosphorylating and stabilizing the PLT1/2 proteins. SOS2-mediated PLT1/2 phosphorylation maintains meristem activity and primary

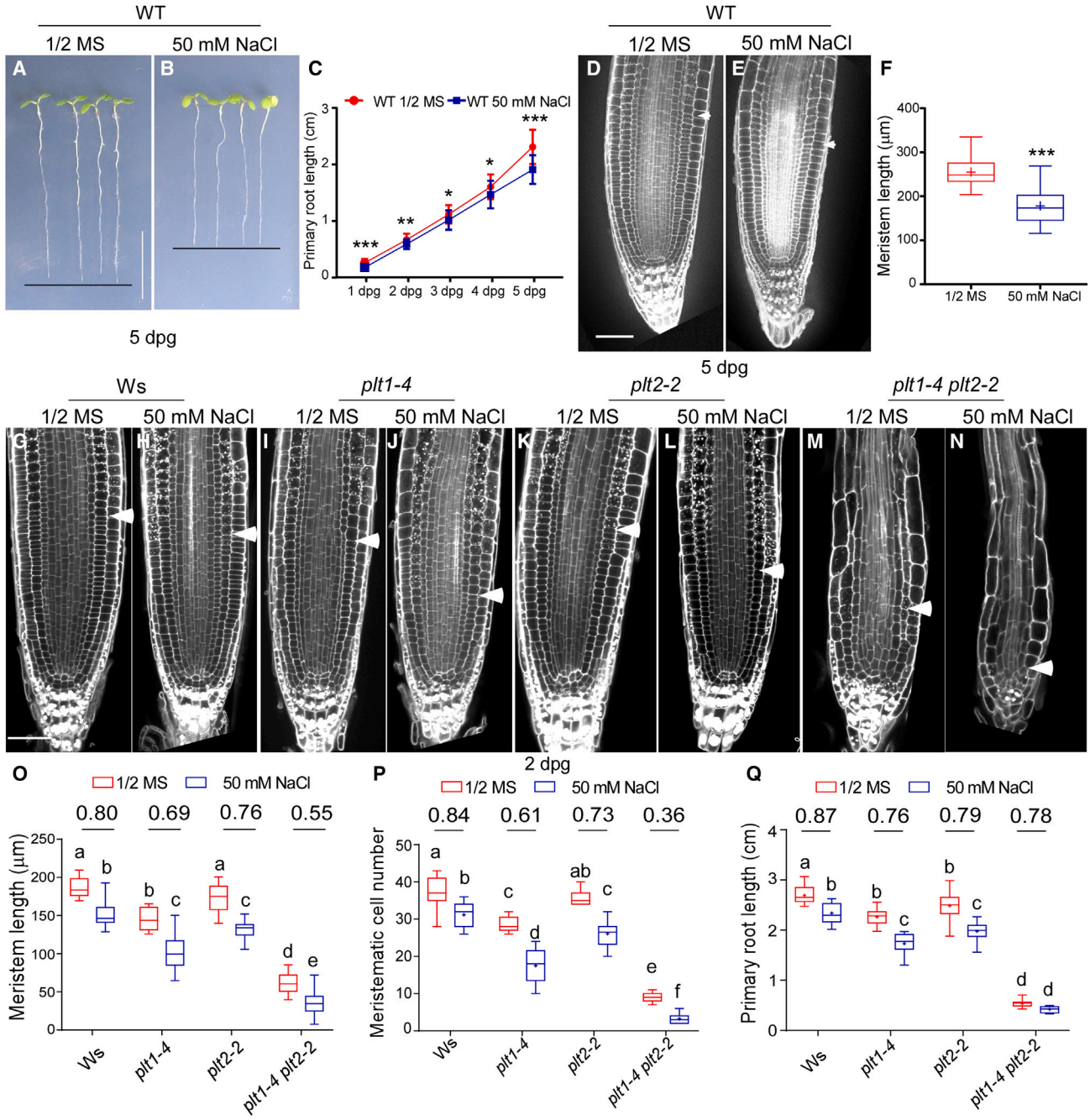


**Figure 1. PLT1/2-regulated meristem maintenance is important for root growth under salt stress**

(A and B) Camera images of *Arabidopsis* wild-type (WT) Col-0 seedlings without (A) or with (B) (hereafter ±) NaCl treatment at 5 days post germination (dpg). Black lines represent position of primary root tips. 1/2 MS: 1/2 MS plus 1% sucrose and 0.8% agar. Scale bars, 1 cm.

(C) Primary root length of WT ± NaCl treatment from 1 to 5 dpg. Data represent mean ± SD (standard deviation). For each data point, n = 24–30. Student's t test, $^{*}p < 0.05$, $^{**}p < 0.01$, $^{***}p < 0.001$.

(D and E) Confocal images of WT root meristem ± NaCl treatment at 5 dpg. Roots were stained with modified pseudo-Schiff propidium iodide (mPS-PI) and imaged at 5 dpg. White arrowheads indicate the root meristem boundary. Scale bars, 50 μm.

(F) Quantification of WT root meristem length ± NaCl treatment. n = 15–27, Student's t test, $^{***}p < 0.001$.

(G–N) Confocal images of the indicated genotypes ± NaCl treatment at 2 dpg. White arrowheads indicate the root meristem boundary. Scale bars, 50 μm.

(O) Quantification of root meristem length in the indicated genotypes ± NaCl treatment. Numbers above boxplots represent relative root meristem ratios ± NaCl treatment (NaCl treatment divides 1/2 MS). Lowercase letters indicate statistically different groups. (n > 15, two-way ANOVA, $p < 0.01$.)

(P) Quantification of meristematic cell number in the indicated genotypes ± NaCl treatment. Numbers above the boxplots represent relative meristematic cell number ratios ± NaCl treatment. Lowercase letters indicate statistically different groups (n > 15, two-way ANOVA, $p < 0.01$).

*(legend continued on next page)*

root growth under salt stress and also regulates root growth recovery after salt stress mitigation.

## RESULTS

### PLT1/2 are required for root meristem maintenance under salt stress

We germinated wild-type (WT) Col-0 *Arabidopsis* seeds on 1/2 MS medium with or without 50 mM NaCl in a time course analysis and confirmed that both the primary root growth and the root meristem length were reduced under salt stress compared with control (Figures 1A–1F). We explored the roles of PLT1/2 and SHR/SCR in salt stress and observed the primary root growth and the root meristem length of *plt1/2*, *shr*, and *scr* mutants with or without salt treatment. After 50 mM salt treatment, *shr-2* and *scr-3* mutants showed similar reduction of the primary root length, meristem length, and meristematic cell number compared with Col-0 (primary root length reduction: Col-0, 14%; *shr-2*, 12%; *scr-3*, 14%; meristem length reduction: Col-0, 27%; *shr-2*, 16%; *scr-3*, 15%; meristematic cell number reduction: Col-0, 16%; *shr-2*, 15%; *scr-3*, 20%) (Figures S1D–S1F, S1H, and S1I). Intriguingly, both the *plt1-4* and the *plt2-2* single mutants, and the *plt1-4 plt2-2* double mutant exhibited enhanced inhibition of primary root growth, meristem length, and meristematic cell number after salt treatment compared with WT (primary root length reduction: Wassilewskija (Ws), 13%; *plt1-4*, 24%; *plt2-2*, 21%; *plt1-4 plt2-2*, 22%; meristem length reduction: Ws, 20%; *plt1-4*, 31%; *plt2-2*, 24%; *plt1-4 plt2-2*, 45%; meristematic cell number reduction: Ws, 16%; *plt1-4*, 39%; *plt2-2*, 27%; *plt1-4 plt2-2*, 64%) (Figures 1G–1Q and S1A). We observed enhanced inhibition of primary root length of the *plt1*, *plt2* single mutants, and the *plt1-4 plt2-2* double mutants with higher concentrations of NaCl (100 mM NaCl), but the primary root length of *shr-2* and *scr-3* mutants did not decrease further compared with 50 mM NaCl treatment, suggesting that *plt1-4*, *plt2-2*, and *plt1-4 plt2-2* are sensitive to salt, but *shr-2* and *scr-3* are less sensitive to salt treatment (primary root length reduction: Ws, 30%; *plt1-4*, 40%; *plt2-2*, 39%; *plt1-4 plt2-2*, 45%; Col-0, 25%; *shr-2*, 14%; *scr-3*, 13%) (Figures S1C and S1J). The average cell length in the differentiation zone was not affected by 50 mM NaCl treatment in any genotype (Figures S1B and S1G), indicating that 50 mM NaCl treatment does not reduce differentiated root cell elongation. These results suggest that PLT1/2 are required for root meristem maintenance after salt treatment.

### SOS2 maintains the root meristem and regulates PLT1/2 protein levels under salt stress

SOS2 plays a key role in ion homeostasis under salt stress. The salt-hypersensitive mutant *sos2-2* showed an enhanced reduction of primary root growth and meristem size after salt treatment for 24 h compared with WT (Figures 2A–2E and S2A–S2C). Consistently, expression of the G2/M phase cell cycle marker *pCYCB1;1::*green fluorescent protein (GFP) was also decreased in the *sos2-2* mutant after salt treatment (Figures S2D–S2F). To examine whether SOS2 regulates root meristem maintenance through the PLT pathway, we introduced the promoter fusin lines *PLT1pro::*cyan fluorescent protein (CFP), *PLT2pro::CFP*, and the protein fusion lines *PLT1pro::PLT1*-yellow fluorescent protein (YFP) and *PLT2pro::PLT2-YFP*, into the *sos2-2* mutant background. *PLT1pro::CFP* and *PLT2pro::CFP* signals in the root meristem were comparable in *sos2-2* and WT during the time course with and without salt treatment (Figures S2G–S2J). Consistent with a previous report,[38] real-time quantitative PCR experiments also showed that *PLT1/2* transcripts were similar in WT and *sos2-2* mutant background after salt treatment over time (Figures S2K and S2L). The YFP signals of PLT protein fusions in *sos2-2* and WT background were comparable without salt treatment. Interestingly, the YFP signals were pronouncedly reduced in *sos2-2* with salt treatment compared with 1/2 MS (Figures 2F–2O). These results indicate that SOS2 regulates PLT1/2 at the post-transcriptional level to regulate root meristem maintenance under salt stress.

### SOS2 interacts with and phosphorylates PLT1/2 proteins by regulating their stability under salt stress

To investigate whether SOS2 directly regulates PLT1/2, we examined the interaction between SOS2 and PLT1/2. Firefly luciferase (LUC) complementation imaging assays in *Nicotiana benthamiana* showed that both PLT1 and PLT2 interacted with SOS2 in planta (Figures 3A and S3A). Split-YFP assays confirmed their interaction in the nucleus (Figures 3B and S3B). We hypothesized that PLT1/2 might be substrates of SOS2, and we purified recombinant His-SOS2 and performed *in vitro* phosphorylation assays. His-SOS2 could phosphorylate maltose binding protein (MBP)-PLT1 and MBP-PLT2 but could not phosphorylate the MBP protein itself (Figures 3C, S3C, and S3D). We next split the PLT1/2 proteins into three functional domains (N-terminal, central, and C-terminal) and found that the C-terminal domains of the recombinant MBP-PLT1/2 (PLT1 381–574 aa; PLT2 389–568 aa) were strongly phosphorylated after incubation with His-SOS2, respectively (Figures S3E–S3G). We explored the PLT1/2 phosphorylation sites through mass spectrum analysis and also examined data from Arabidopsis Protein Phosphorylation Site Database (Figures S3H and S3I). Four amino acid residues of PLT1, Ser401-Thr402-Ser403-Ser404 (hereafter PLT1$^{S4}$), homologous to PLT2 Ser411-Ser412-Ser413 (hereafter PLT2$^{S3}$), were selected as potential phosphorylation sites by SOS2 (Figures S3E and S3I). We mutated these amino acids into alanine (PLT1$^{S4A}$ and PLT2$^{S3A}$) and performed *in vitro* phosphorylation assays. We found reduced phosphorylation of MBP-PLT1$^{S4A}$ and MBP-PLT2$^{S3A}$ by His-SOS2 (Figures 3C and S3D), suggesting that SOS2 phosphorylates PLT1/2 at least partially through these sites. In summary, these results showed that SOS2 interacts with the

(Q) Quantification of primary root length in the indicated genotypes ± NaCl treatment. Numbers above boxplots represent relative primary root length ratios ± NaCl treatment. Lowercase letters indicate statistically different groups ($n > 10$, two-way ANOVA, $p < 0.01$).
Boxplots depict the minimum to maximum. Different genotypes were germinated on 1/2 MS medium ± 50 mM NaCl.
See also Figure S1.

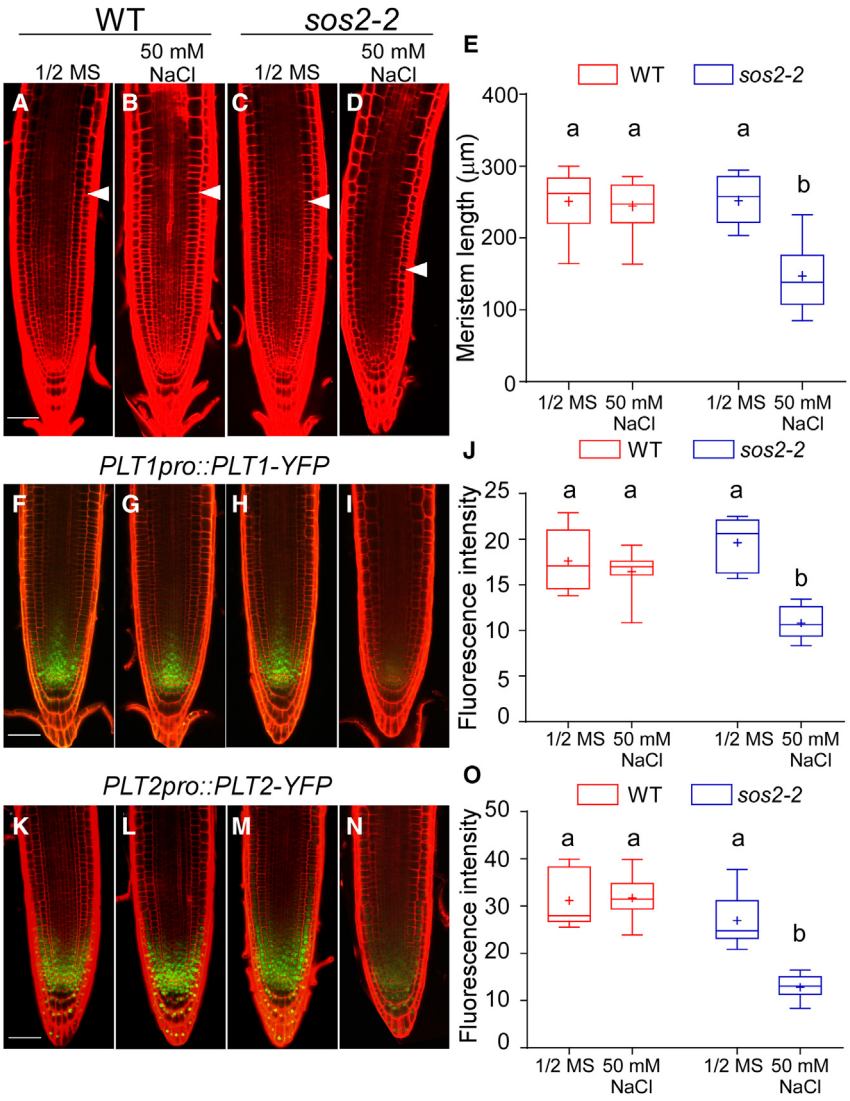


**Figure 2. SOS2 regulates root meristem activity by maintaining the PLETHORA (PLT) 1/2 proteins**

(A–D, F–I, and K–N) Confocal images of the root meristem of WT (*gl1*) (A and B), *sos2-2* mutant (C and D), *PLT1pro::PLT1-YFP gl1* (F and G), *PLT1pro::PLT1-YFP sos2-2* (H and I), *PLT2pro::PLT2-YFP gl1* (K and L), and *PLT2pro::PLT2-YFP sos2-2* (M and N) ± 50 mM NaCl for 24 h. White arrowheads indicate the root meristem boundary. Scale bars, 50 μm.

(E) Quantification of the root meristem length in WT (*gl1*) and *sos2-2* ± NaCl treatment. Lowercase letters indicate statistically different groups (n = 11–20, one-way ANOVA, $p < 0.001$).

(J and O) Quantification of the PLT1-YFP and PLT2-YFP fluorescence intensity ± NaCl treatment in WT and *sos2-2*, respectively. Lowercase letters indicate statistically different groups (n > 8, one-way ANOVA, $p < 0.001$).

Boxplots depict the minimum to maximum.

See also Figure S2.

PLT1/2 proteins, and SOS2 phosphorylates PLT1/2 through their C-terminal domains.

We investigated whether phosphorylation of PLT1/2 via SOS2 alters their protein stability by performing degradation assays *in vivo* and *in vitro*. *PLT1pro::PLT1-YFP* and *PLT2pro::PLT2-YFP* lines in WT and *sos2-2* background were treated with or without NaCl and tested by immunoblot analysis. Both the abundance of PLT1-YFP and PLT2-YFP were decreased in *sos2-2* under salt treatment compared with WT (Figures 3D and S4A). LUC complementation imaging assays showed that SOS2 could interact with PLT1/2$^{WT}$ and the phospho-mimetic form PLT1$^{S4E}$/PLT2$^{S3E}$ but could only weakly interact with the phospho-inactive PLT1$^{S4A}$/PLT2$^{S3A}$ (Figures 3J and S4B). We performed cell-free assays to further confirm SOS2's effect on PLT1/2 stability *in vitro*. Without salt treatment, the recombinant MBP-PLT1/2 proteins showed similar stability in protein extracts of the *sos2-2* mutant compared with WT (Figures S4C and S4D). Recombinant MBP-PLT1/2 proteins were stable in WT extracts under salt stress but were degraded quickly in *sos2-2* extracts with salt treatment (Figures 3E and S4E). When the proteasome inhibitors MG132 and MG115 were added, respectively, degradation of PLT1/2 was strongly inhibited in *sos2-2* extracts with salt (Figures 3F, 3G, S4F, and S4G). Interestingly, the autophagy inhibitor 3MA (3-methyladenine) also inhibited PLT1/2 degradation (Figures 3H and S4H), indicating that PLT1/2 were degraded not only through the 26S proteasome after salt treatment but also through the autophagy pathway. We next explored the function of PLT1/2 phosphorylation on their protein stability. The phospho-mimetic PLT1$^{S4D}$/PLT2$^{S3E}$ proteins were more stable than the phospho-inactive PLT1$^{S4A}$/PLT2$^{S3A}$ proteins under salt stress in *sos2-2* mutant (Figures 3I, S4I, and S4J). We further took microscopy images of PLT protein localization (WT and phospho-mimic/knockout variants) with and without salt stress, respectively. The images indicate that salt treatment does not affect PLT1/2 localization (Figures S4K–S4V). Taken together, these data indicate that SOS2-mediated phosphorylation on PLT1$^{S4}$/PLT2$^{S3}$ represses protein degradation under salt stress.

## PLT1/2 phosphorylation maintains root meristem activity under salt stress

We generated the phospho-mimetic *pPLT1:: GFP-PLT1$^{S4D}$* and *pPLT2::GFP-PLT2$^{S3E}$* lines, and the phospho-inactive *pPLT1:: GFP-PLT1$^{S4A}$* and *pPLT2::GFP-PLT2$^{S3A}$* lines, and combined them with the *sos2-2* mutant, respectively. We found that *pPLT1::GFP-PLT1$^{S4D}$ sos2-2* and *pPLT2::GFP-PLT2$^{S3E}$ sos2-2* partially restored meristem and primary root length reduction of *sos2-2* with salt treatment (Figures 4A–4G and S5A–S5G). On the other hand, *pPLT1::GFP-PLT1$^{S4A}$ sos2-2* and *pPLT2::GFP-PLT2$^{S3A}$ sos2-2* exhibited similar reduction of meristem and primary root length compared with *sos2-2* with salt treatment

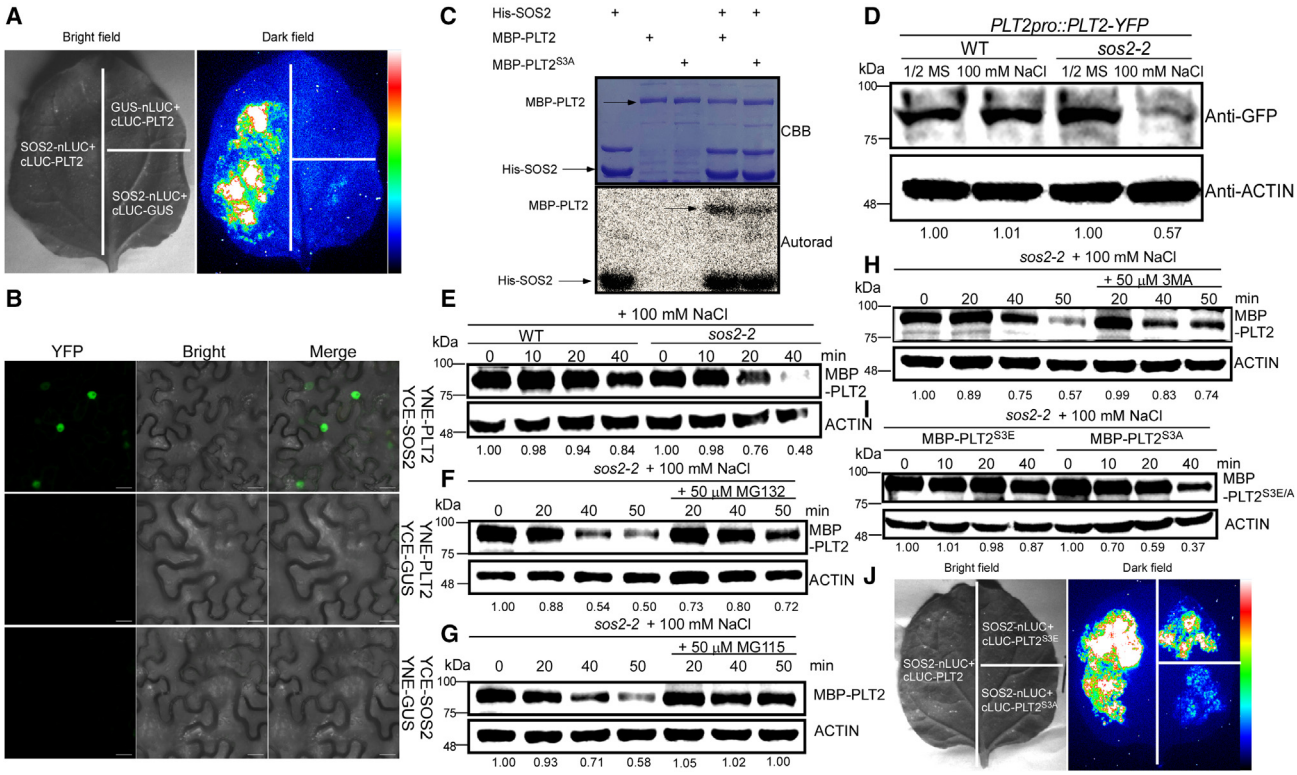


**Figure 3. SOS2 interacts with PLT1/2 and enhances PLT1/2 protein stability through phosphorylation under salt stress**

(A) Split-Luc assays showing that PLT2 interacts with SOS2 in *N. benthamiana*. Indicated constructs were transiently expressed in *N. benthamiana*, and the GUS (β-glucuronidase) protein was served as a negative control. Pseudocolor bar shows the range of luminescence intensity. Nluc, N-terminal fragment of firefly luciferase; Cluc, C-terminal fragment of firefly luciferase.

(B) Bimolecular fluorescence complementation assays in *N. benthamiana* showing that PLT2 interacts with SOS2 in the nucleus. YCE, C-terminal YFP fragment; YNE, N-terminal YFP fragment. The GUS protein was served as a negative control. Scale bars, 50 μm.

(C) *In vitro* kinase assays showing that SOS2 phosphorylates PLT2 at three phosphorylation sites (Ser-411, Ser-412, and Ser-413, hereafter PLT2$^{S3}$). Top panel shows Coomassie brilliant blue (CBB)-stained SDS-PAGE gel containing His-SOS2, MBP-PLT2, and the mutated PLT2 (MBP-PLT2$^{S3A}$, to Ala) proteins. Bottom panel shows autoradiography (Autorad), indicating SOS2 autophosphorylation and MBP-PLT2 and MBP-PLT2$^{S3A}$ phosphorylation. Black arrows point to the indicated recombinant proteins.

(D) Immunoblot analysis of the PLT2-YFP protein levels in the indicated genotypes ± NaCl treatment. *PLT2pro::PLT2-YFP* and *PLT2pro::PLT2-YFP sos2-2* seedlings were grown on 1/2 MS medium for 6 days and treated ± 100 mM NaCl for 24 h. ACTIN was used as a control. kDa, kilodalton.

(E) Cell-free degradation assays showing that MBP-PLT2 is degraded faster in *sos2-2* mutant under salt treatment compared with WT. Recombinant MBP-PLT2 proteins (100 ng/100 μL total cell-free extracts) were added to the extracts prepared from 7 dpg WT and *sos2-2* seedlings with salt treatment for the indicated time. MBP-PLT2 proteins were detected with anti-MBP antibody. ACTIN was used as a control.

(F–H) Cell-free degradation assays showing that MG132 (F), MG115 (G), or 3MA (H) treatment inhibits MBP-PLT2 degradation in *sos2-2* under salt stress. The extracts prepared from *sos2-2* seedlings at 7 dpg with salt treatment were incubated with recombinant MBP-PLT2 with or without 50 μm MG132, MG115, or 3MA for the indicated time.

(I) Cell-free degradation assays showing that MBP-PLT2$^{S3E}$ proteins are degraded slower than MBP-PLT2$^{S3A}$ in *sos2-2* with salt treatment. The recombinant MBP-PLT2$^{S3E}$ and MBP-PLT2$^{S3A}$ proteins were added to extracts prepared from 7 dpg *sos2-2* seedlings with salt treatment for the indicated time.

(J) Split-Luc assays showing that PLT2$^{S3E}$-SOS2 interaction is stronger than PLT2$^{S3A}$-SOS2 in *N. benthamiana*. Nluc, N-terminal fragment of firefly luciferase; Cluc, C-terminal fragment of firefly luciferase.

See also Figures S3 and S4.

(Figures 4A–4G and S5A–S5G). Consistently, *pPLT1::GFP-PLT1$^{S4A}$ sos2-2* and *pPLT2::GFP-PLT2$^{S3A}$ sos2-2* lines showed enhanced reduction of the GFP expression compared with *pPLT1::GFP-PLT1$^{S4D}$ sos2-2* and *pPLT2::GFP-PLT2$^{S3E}$ sos2-2* lines with salt treatment (Figures 4A, 4C, S5A, and S5E).

To confirm whether the SOS2-PLT1/2 module regulates root meristem cell division upon salt treatment, we performed 5-ethynyl-20-deoxyuridine (EdU) staining of root meristems in WT (*gl1*), *sos2-2*, and *sos2-2* PLT1/2 phospho-mimetic and phospho-inactive lines. The number of EdU-labeled cells was largely reduced in the *sos2-2* mutant after salt treatment. Confocal images and quantification of the number of EdU-labeled cells both showed that the phospho-mimetic version of PLT1/2 (PLT1$^{S4D}$/PLT2$^{S3E}$) could partly rescue the decreased EdU-labeled cell number in *sos2-2*, indicating that the SOS2-PLT1/2 module regulates root meristem cell division under salt stress (Figures 4H, 4I, S5H, and S5I). Furthermore, root tip RNA-seq data showed that transcripts encoding the number of cell division regulators were significantly decreased in *sos2-2* compared with WT under salt stress (Figure S5J; Table S2).

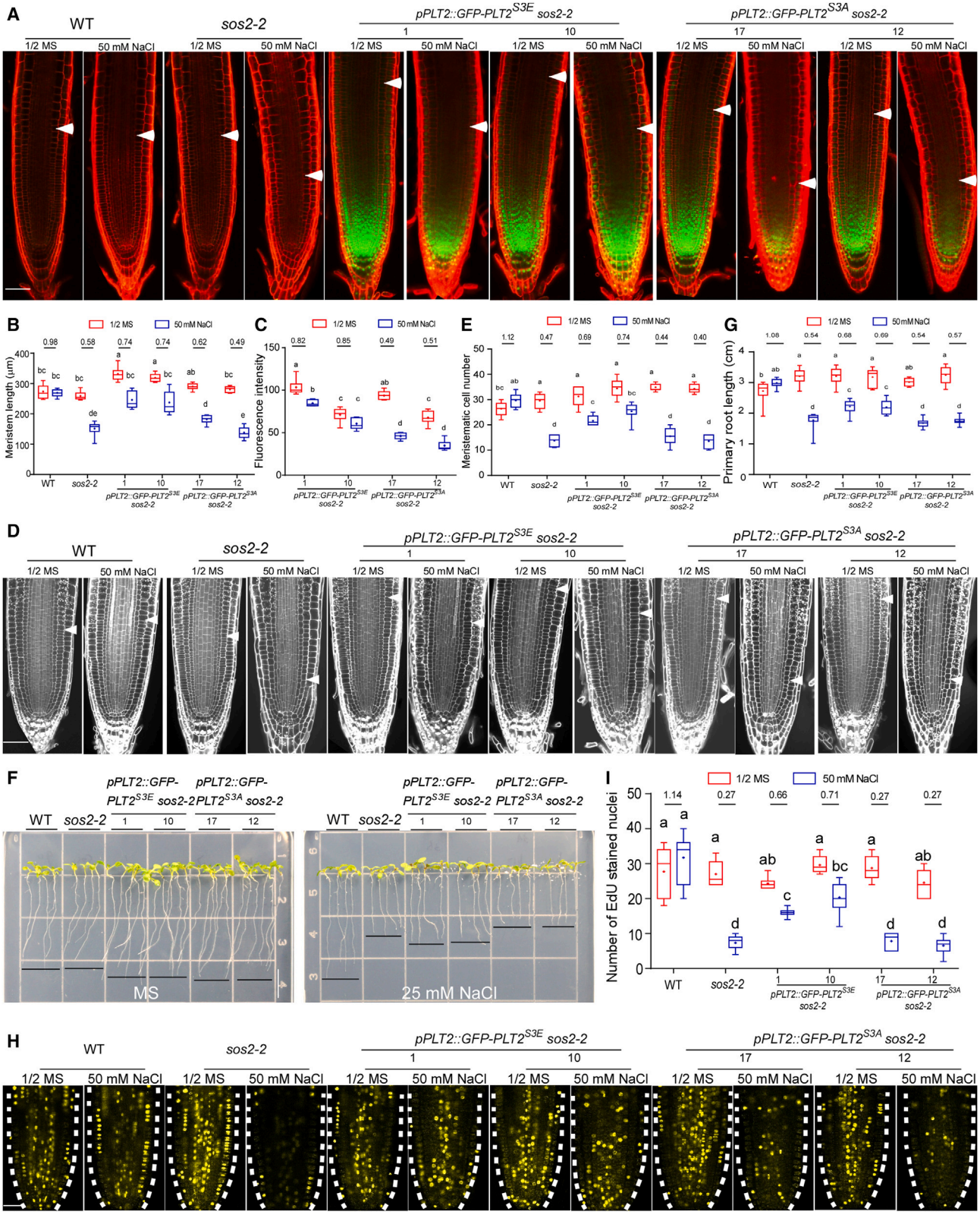


*(legend on next page)*

Consistent with the RNA-seq data, *CYCB1;1*, *CCS52A*, and *CYCD3;3* gene expression was significantly reduced in *sos2-2* after salt treatment. Interestingly, the phospho-mimetic version of PLT1/2, but not the phospho-inactive version of PLT1/2, complemented the cell cycle gene reduction in *sos2-2* lines after salt treatment (Figures S5K–S5M). To investigate whether SCN activity was affected in these genotypes under salt stress, we performed modified pseudo-Schiff propidium iodide (mPS-PI) staining and took confocal images of the SCN region in WT (*gl1*), *sos2-2*, PLT1/2$^{S4E/A}$ *sos2-2* lines (Figures S6A–S6C). We did not observe obvious changes in the SCN organization and the QC cell number in different genotypes with and without salt treatment. In summary, SOS2-PLT1/2 regulates cell division in root meristem under salt stress.

To further confirm whether the PLT1 and PLT2 phospho-mimetics additively enhance resistance to higher salt stress, we crossed the *pPLT1::GFP-PLT1$^{S4D}$ sos2-2* with *pPLT2::GFP-PLT2$^{S3E}$ sos2-2*. The *pPLT1::GFP-PLT1$^{S4D}$ pPLT2::GFP-PLT2$^{S3E}$ sos2-2* lines could better restore *sos2-2* primary root and meristem length both under 25 mM NaCl and 50 mM NaCl treatment, respectively, compared with their parental lines (Figures S6D–S6G), indicating an additive role of PLT1 and PLT2 under salt stress.

We next performed complementation tests and transformed *pPLT1:: GFP-PLT1$^{S4D}$*, *pPLT2::GFP-PLT2$^{S3E}$*, *pPLT1::GFP-PLT1$^{S4A}$*, *pPLT2::GFP-PLT2$^{S3A}$*, *pPLT1::GFP-PLT1*, and the *pPLT2::GFP-PLT2* constructs into the *plt1-4 plt2-2* double-mutant background and observed that all constructs rescued the meristem and root length defect of *plt1-4 plt2-2* without salt stress (Figures 5 and S7). Interestingly, we found an enhanced reduction of meristem, primary root length, and GFP intensity of *pPLT1::GFP-PLT1$^{S4A}$ plt1-4 plt2-2* and *pPLT2::GFP-PLT2$^{S3A}$ plt1-4 plt2-2* lines after salt treatment, compared with the corresponding phospho-mimetic lines (Figures 5 and S7). Taken together, these results suggest that PLT1$^{S4}$/PLT2$^{S3}$ phosphorylation is required for root meristem maintenance with salt treatment.

## PLT1/2-mediated root meristem maintenance is required for growth recovery after salt stress

To test the salt resistance of PLT phospho-mimetic and phospho-inactive lines at a longer timescale, we performed a soil experiment with NaCl watered (Figures S6H–S6J), and we observed that PLT1/2 phospho-mimetic version in *sos2-2* showed more resistance with extended salt stress. Instead, phospho-inactive versions of PLT1/2 in *sos2-2* exhibited similar phenotypes compared with *sos2-2* in soil, suggesting that more stable PLT1/2 proteins under salt stress could also help whole plants to cope with salt stress in soil.

We next asked whether the stability of PLT1/2, which is regulated by SOS2-mediated phosphorylation, affects the recovery of primary root growth after salt stress alleviation. We sowed WT, *sos2-2*, *pPLT1::GFP-PLT1$^{S4D}$ sos2-2*, *pPLT1::GFP-PLT1$^{S4A}$ sos2-2*, *pPLT2::GFP-PLT2$^{S3E}$ sos2-2*, and *pPLT2::GFP-PLT2$^{S3A}$ sos2-2* seeds on 1/2 MS medium with or without NaCl, and subsequently, seedlings at 4 days post germination (dpg) were transferred to 1/2 MS medium for recovery. 1 day after growth recovery, we found that root meristem length in *sos2-2*, *pPLT1::GFP-PLT1$^{S4A}$ sos2-2*, and *pPLT2::GFP-PLT2$^{S3A}$ sos2-2* lines was still shorter compared with WT. Consistently, we also observed a lower expression of *GFP-PLT1$^{S4A}$* and *GFP-PLT2$^{S3A}$* 1 day after recovery growth, compared with mock treatment (Figures 6A–6D, 6G, 6H, 6K, and 6L). On the other hand, both the root meristem length of *pPLT1::GFP-PLT1$^{S4D}$ sos2-2* and *pPLT2::GFP-PLT2$^{S3E}$ sos2-2* lines and the expression of GFP-PLT1$^{S4D}$ and GFP-PLT2$^{S3E}$ were recovered and similar to that of mock treatments (Figures 6A–6F, 6I, and 6J). Time course analysis further confirmed that meristem length and the primary root growth of *sos2-2* and the phospho-inactive *pPLT1::GFP-PLT1$^{S4A}$ sos2-2* and *pPLT2::GFP-PLT2$^{S3A}$ sos2-2* lines recovered slower than that of WT and phospho-mimetic *pPLT1::GFP-PLT1$^{S4D}$ sos2-2* and *pPLT2::GFP-PLT2$^{S3E}$ sos2-2* lines (Figures 6M–6S). Extended recovery experiments revealed that *sos2-2* and the phospho-inactive *pPLT1::GFP-PLT1$^{S4A}$ sos2-2* and *pPLT2:: GFP-PLT2$^{S3A}$ sos2-2* lines could not recover well after pulse salt

**Figure 4. Phosphorylation of PLT2 is required for SOS2-mediated meristem maintenance and primary root growth under salt stress**

(A) Confocal images of root meristem of WT (*gl1*), *sos2-2*, *pPLT2::GFP-PLT2$^{S3E}$ sos2-2*, and *pPLT2::GFP-PLT2$^{S3A}$ sos2-2* ± NaCl treatment. Seedlings at 4 dpg were transferred to 1/2 MS or 50 mM NaCl medium for 24 h. Two individual transgenic lines are shown for each construct. White arrowheads indicate the root meristem boundary. Scale bars, 50 μm.

(B and C) Quantification of the root meristem length (B) and fluorescence intensity (C) of the indicated genotypes ± NaCl treatment. Numbers above boxplots represent relative root meristem length (B) or fluorescence intensity (C) ratios ± NaCl treatment, respectively. Data represent 3 independent experiments with >8 replicates per treatment in each genotype. Lowercase letters indicate statistically different groups (two-way ANOVA, $p < 0.01$).

(D) mPS-PI confocal images of root meristem of WT (*gl1*), *sos2-2*, *pPLT2::GFP-PLT2$^{S3E}$ sos2-2*, and *pPLT2::GFP-PLT2$^{S3A}$ sos2-2* ± NaCl treatment. Seedlings at 2 dpg were transferred to 1/2 MS or 50 mM NaCl medium for 24 h. Two individual transgenic lines are shown for each construct. Scale bars, 50 μm.

(E) Quantification of the meristematic cell number of the indicated genotypes ± NaCl treatment. Numbers above boxplots represent relative meristematic cell number ratios ± NaCl treatment, respectively. Lowercase letters indicate statistically different groups ($n > 10$, two-way ANOVA, $p < 0.01$).

(F) Camera images of WT (*gl1*), *sos2-2*, *pPLT2::GFP-PLT2$^{S3E}$ sos2-2*, and *pPLT2::GFP-PLT2$^{S3A}$ sos2-2* ± NaCl treatment. The seedlings at 2 dpg were treated with or without 25 mM NaCl for 3 days. Black lines represent position of primary root tips. Scale bars, 1 cm.

(G) Quantification of the primary root length in the indicated genotypes ± NaCl treatment. Numbers above the boxplots represent relative primary root length ratios ± NaCl treatment. Data represent 3 independent experiments with >8 replicates per treatment in each genotype. Lowercase letters indicate statistically different groups (two-way ANOVA, $p < 0.01$).

(H) Confocal images of EdU-labeled roots meristem of WT (*gl1*), *sos2-2*, *pPLT2::GFP-PLT2$^{S3E}$ sos2-2* and *pPLT2::GFP-PLT2$^{S3A}$ sos2-2* ± NaCl treatment. Seedlings at 2 dpg were transferred to 1/2 MS or 50 mM NaCl medium for 24 h with EdU staining kits. White dashed lines represent the meristem zone. Scale bars, 50 μm.

(I) Quantification of the number of EdU-labeled cells in the indicated genotypes ± NaCl treatment. The number of EdU-labeled cells was counted in the epidermis, cortex, and endodermis cell layers on both sides of the root. Numbers above the boxplots represent relative number of EdU-labeled cells ratios ± NaCl treatment. Lowercase letters indicate statistically different groups ($n > 8$, two-way ANOVA, $p < 0.01$).

See also Figures S5 and S6 and Table S2.

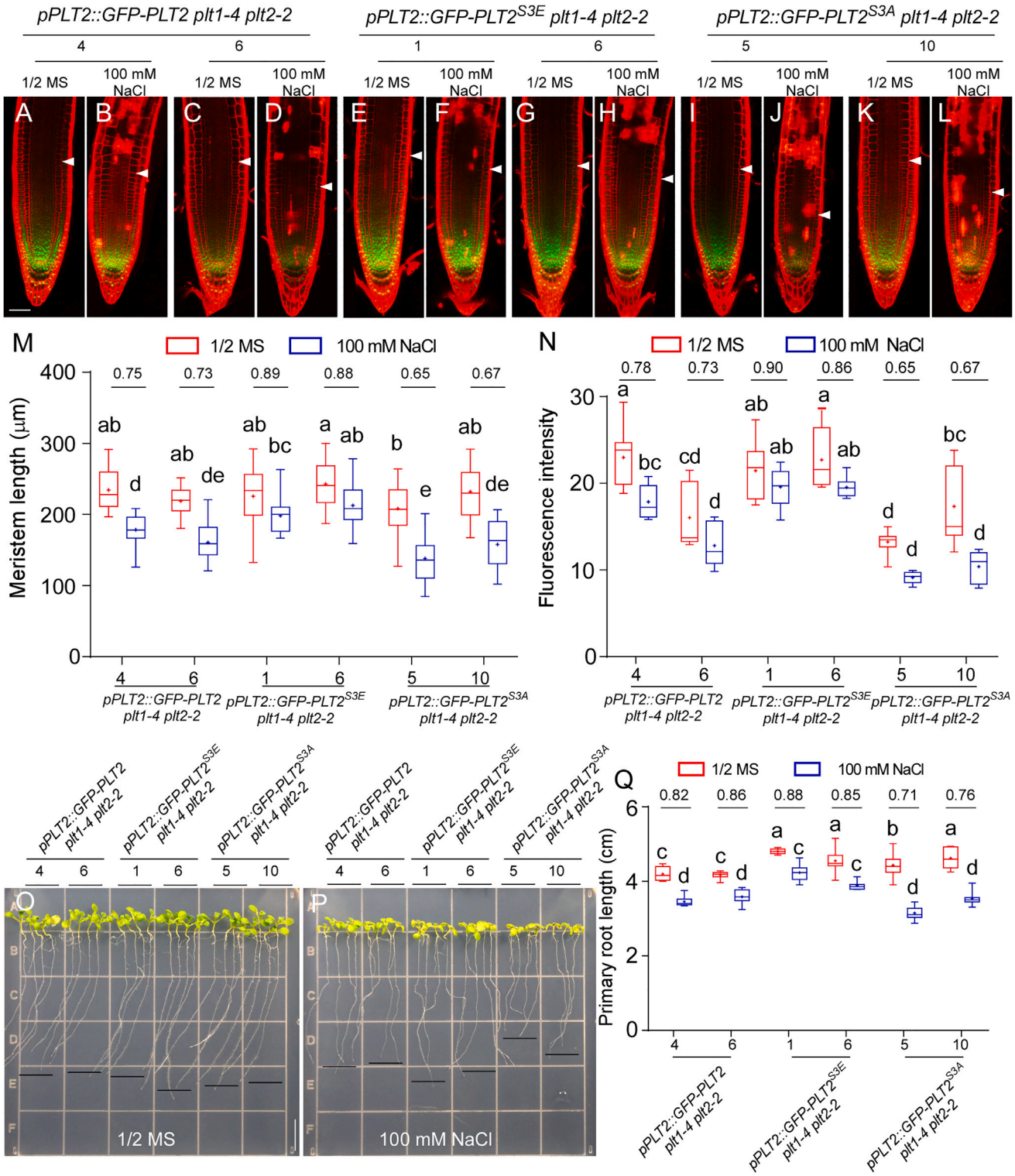


**Figure 5. Complementation analysis showing better complementation of phospho-mimetic PLT2 forms in *plt1-4 plt2-2* compared with the phospho-inactive version after salt stress**

(A–L) Confocal images of root meristem of *pPLT2::GFP-PLT2 plt1-4 plt2-2* (A–D), *pPLT2::GFP-PLT2$^{S3E}$ plt1-4 plt2-2* (E–H), and *pPLT2::GFP-PLT2$^{S3A}$ plt1-4 plt2-2* (I–L) ± NaCl treatment. Seedlings at 4 dpg were treated with 100 mM NaCl for 24 h. Two individual transgenic lines were shown for each construct. White arrowheads indicate the root meristem boundary. Scale bars, 50 μm.

*(legend continued on next page)*

treatment, whereas both the shoots and roots of phospho-mimetic *pPLT1::GFP-PLT1*$^{S4D}$ *sos2-2* and *pPLT2::GFP-PLT2*$^{S3E}$ *sos2-2* lines recovered significantly better compared with *sos2-2* and the phospho-inactive *pPLT1::GFP-PLT1*$^{S4A}$ *sos2-2* and *pPLT2::GFP-PLT2*$^{S3A}$ *sos2-2* lines (Figures 6T–6Y). In summary, our results indicate that SOS2 phosphorylates and stabilizes PLT1/2 under transient salt stress, which helps plant roots and shoots recover faster after salt stress alleviation.

## DISCUSSION

How to keep a balance between growth and stress resistance and shift to rapid post-stress growth are fundamental questions for plants interacting with complex environments. Many studies have revealed the molecular mechanism of root resistance to salt-stress-induced ionic toxicity, osmotic stress, and oxidative stress, but there are very few studies focusing on the maintenance of meristem activity and growth in response to salt stress. In this study, we identify a SOS2-PLT1/2 core protein module that is required for root meristem maintenance under salt stress (Figure 7). Salt-induced SOS2 regulates PLT1 and PLT2 proteins at the post-transcriptional level. SOS2 phosphorylates and stabilizes the PLT1/2 proteins through the conserved motif in the C-terminal domain of the PLT1/2 proteins. Importantly, phosphorylated PLT1/2 maintains the root meristem and root growth under salt stress. SOS2-mediated PLT1/2 phosphorylation also helps plant shoots and roots to recover faster after transient exposure to high salt levels. In summary, we find that root meristem activity must be precisely maintained at a certain level, based on the duration and degree of salt stress, which will help plants balance root growth and salt resistance.

Previous studies show that PLT proteins function as dose-dependent master regulators of root development.[31] Specifically, high levels of PLT activity determine stem cell identity, medium levels promote the mitotic activity of meristematic cells, and lower levels are required for cell differentiation.[31] The gradient of PLT is generated through slow growth dilution and cell-to-cell movement.[32] Our work now reveals how PLT1/2 proteins are regulated at the post-transcriptional level under stress conditions. Importantly, both the phospho-inactive and the phospho-mimetic versions of PLT1 and PLT2 rescued meristem and root length defects of *plt1-4 plt2-2* under normal conditions, but only the phospho-inactive version exhibited enhanced reduction of meristem and root growth under salt stress, suggesting that SOS2-mediated PLT1$^{S4}$/PLT2$^{S3}$ phosphorylation is necessary for root meristem maintenance under salt stress. Consistently, RNA-seq and EdU experiments also showed that cell division gene expression was significantly reduced in *sos2-2* mutants, and the phosphorylated version of PLT1/2 could largely restore cell division in the root meristem, suggesting that the SOS2-PLT1/2 module regulates meristem cell division to maintain meristem activity under salt stress. It is worth noting that the PLT1$^{S4}$/PLT2$^{S3}$ phosphorylation sites are only conserved between PLT1 and PLT2, but not in other PLTs, suggesting that PLT1 and PLT2 are specific targets of the SOS pathway in root meristem maintenance under salt stress.

When plants are subjected to environmental changes, post-transcriptional regulation could be a faster response mechanism than transcriptional regulation. A recent study also reported a TOP1$\alpha$-TOR-PLT2 module that maintains root tip homeostasis in response to sugar.[39] The transcriptional regulation of PLT genes has significantly delayed effects on PLT protein levels.[32] Because the level of PLT proteins determines the ability of meristematic cells to remain division competent, stabilizing the master regulators of root development (e.g., PLT1/2) at the protein level is an effective mechanism for plants to maintain the root meristem and, therefore, the capacity to resume root growth after salt stress.

The SOS pathway is important for plants to export $Na^+$, alleviating ion toxicity in the roots. There are several clues about the SOS signaling pathway regulating root growth plasticity in response to salt stress.[7,20] Interestingly, we found that the phospho-mimetic version of PLT1 and PLT2 could partly rescue the reduction of meristem and primary root growth in *sos2-2* under mild salt stress, positioning PLT1/2 genetically downstream of SOS2 in salt-mediated primary root growth. Mild NaCl concentrations were used in this study, whereas SOS2 kinase activity is induced in a NaCl concentration-dependent manner[11]; hence, further studies should resolve how root meristem differentiation is regulated by SOS2-PLT1/2 protein module in higher salt conditions.

Our studies connect directly SOS2 to the PLT1/2 master regulators in root development and reveal a critical role of SOS2 in salt-mediated root meristem maintenance. Our results open a window to further understand trade-offs between plant growth and stress response and to comprehend how plants successfully cope with their environment.

### Limitations of the study

We elucidate that salt-activated SOS2 phosphorylates PLT1/2 and the phosphorylated PLT1/2 maintain root meristem to keep primary root growth both under salt stress and during recovery from salt alleviation. Additional studies into the mechanisms of PLT pathway in maintaining root meristem under salt stress will be a critical next step in future studies. In specific, what are the different downstream targets of phosphorylated

(M and N) Quantification of meristem length (M) and fluorescence intensity (N) in the indicated genotypes ± NaCl treatment. Numbers above the boxplots represent relative ratios ± NaCl treatment. Data represent 3 independent experiments with >8 replicates per treatment in each genotype. Lowercase letters indicate statistically different groups (two-way ANOVA, $p < 0.01$).

(O and P) Camera images of *pPLT2::GFP-PLT2 plt1-4 plt2-2*, *pPLT2::GFP-PLT2*$^{S3E}$ *plt1-4 plt2-2*, and *pPLT2::GFP-PLT2*$^{S3A}$ *plt1-4 plt2-2* ± NaCl treatment. Black lines represent position of primary root tips. Scale bars, 1 cm.

(Q) Quantification of the primary root length in the indicated genotypes ± NaCl treatment. Numbers above the boxplots represent relative primary root length ratios ± NaCl treatment. Data represent 3 independent experiments with >8 replicates per treatment in each genotype. Lowercase letters indicate statistically different groups (two-way ANOVA, $p < 0.01$).

See also Figure S7.

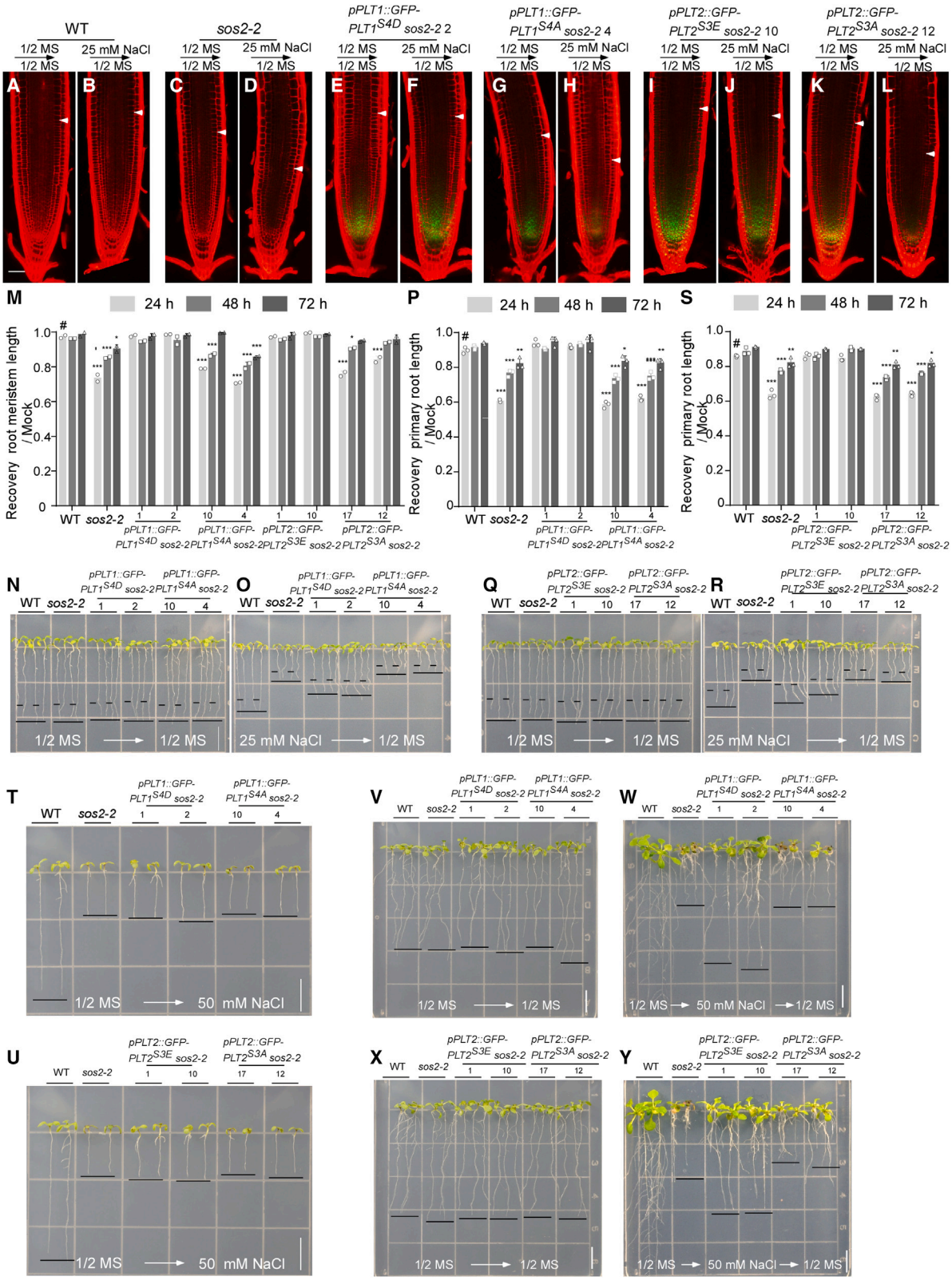


**Figure 6. SOS2-mediated phosphorylation of PLT1/2 promotes primary root growth recovery after salt stress alleviation**

(A–L) Confocal images of root meristem recovery of WT (*gl1*) (A and B), *sos2-2* (C and D), *pPLT1::GFP-PLT1*$^{S4D}$ *sos2-2* (E and F), *pPLT1::GFP-PLT1*$^{S4A}$ *sos2-2* (G and H), *pPLT2::GFP-PLT2*$^{S3E}$ *sos2-2* (I and J), and *pPLT2::GFP-PLT2*$^{S3A}$ *sos2-2* (K and L) after NaCl treatment. Seeds were sown on 1/2 MS ± 25 mM NaCl,

*(legend continued on next page)*

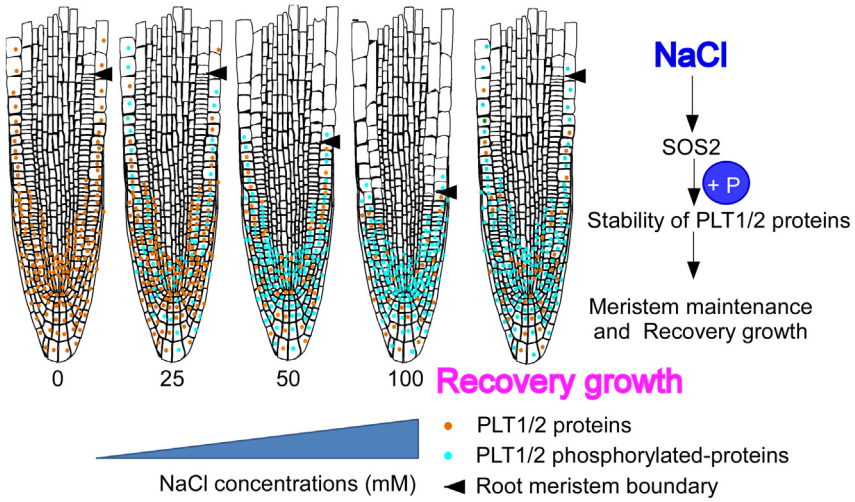


**Figure 7. Model depicting how SOS2-mediated phosphorylation of PLT1/2 promotes plant growth under salt stress and recovery after salt stress alleviation**

Salt activates the SOS2 activity, and SOS2 phosphorylates and stabilizes PLT1/2 proteins. The SOS2-PLT1/2 protein module is important not only for root meristem maintenance under salt stress but also for growth recovery after salt stress alleviation. Orange circles indicate PLT1/2 proteins. Blue circles indicate PLT1/2 phosphorylated proteins. Black arrows indicate root meristem boundary. Blue triangle indicates NaCl concentrations.

and non-phosphorylated versions of PLT1/2 under salt stress, and what are their roles in maintaining root meristem under salt stress? Besides, our data do not exclude that SOS2 may regulate other meristem regulators to maintain meristem activity, such as the SHR/SCR pathway. As our data show that *shr/scr* mutants are less sensitive to salt stress, they are interested in further investigating how SHR/SCR pathway regulates root meristem maintenance under salt stress. Future studies are still needed to delineate how plants sense abiotic stress signaling to regulate primary root development to adapt to environmental changes. Furthermore, how the PLT1/2 protein stability is regulated is required for further study.

## STAR★METHODS

Detailed methods are provided in the online version of this paper and include the following:



and at 4 dpg seedlings were transferred to 1/2 MS for 24 h before imaging. NaCl → 1/2 MS represents recovery after salt treatment, and 1/2 MS → 1/2 MS represents mock treatment. White arrowheads indicate the root meristem boundary. Scale bars, 50 μm.

(M) Time series quantification of relative root meristem length in the indicated genotypes transferred to 1/2 MS after ± NaCl treatment. Relative meristem length represents the ratios of recovery growth of root meristem length after NaCl treatment (recovery meristem length/mock meristem length). Data represent 2 independent experiments with >8 replicates per treatment in each genotype. (One-way ANOVA, *p < 0.05, **p < 0.01, ***p < 0.001.)

(P and S) Time series quantification of relative primary root recovery growth of the indicated genotypes transferred to 1/2 MS after NaCl treatment. Relative primary root length represents the ratios of recovery growth of primary root length after NaCl treatment (recovery primary root length/mock primary root length). Data represent 3 independent experiments with >8 replicates per treatment in each genotype. (One-way ANOVA, *p < 0.05, **p < 0.01, ***p < 0.001.)

(N–O and Q–R) Camera images of WT (*gl1*), *sos2-2*, *pPLT1::GFP-PLT1$^{S4D}$ sos2-2* and *pPLT1:GFP-PLT1$^{S4A}$ sos2-2*, *pPLT2::GFP-PLT2$^{S3E}$ sos2-2*, and *pPLT2::GFP-PLT2$^{S3A}$ sos2-2* on 1/2 MS or on NaCl transferred to 1/2 MS for recovery growth for 24 h. Seeds were sown on 1/2 MS ± 25 mM NaCl, and the seedlings at 4 dpg were transferred to 1/2 MS medium for recovery for 24 h. Dashed lines represent positions of primary root tips at 0 h after transfer. Black lines represent position of primary root tips. Scale bars, 1 cm.

(T and U) Camera images of WT (*gl1*), *sos2-2*, *pPLT1::GFP-PLT1$^{S4D}$ sos2-2*, *pPLT1:GFP-PLT1$^{S4A}$ sos2-2*, *pPLT2::GFP-PLT2$^{S3E}$ sos2-2*, and *pPLT2::GFP-PLT2$^{S3A}$ sos2-2* seedings. The seedlings at 2 dpg were transferred to 50 mM NaCl for 4 days before imaging. Black lines represent position of primary root tips. Scale bars, 1 cm.

(V–Y) Camera images of WT (*gl1*), *sos2-2*, *pPLT1::GFP-PLT1$^{S4D}$ sos2-2*, and *pPLT1:GFP-PLT1$^{S4A}$ sos2-2*, *pPLT2::GFP-PLT2$^{S3E}$ sos2-2*, and *pPLT2::GFP-PLT2$^{S3A}$ sos2-2* seedings for the indicated treatments. Seeds were sown on 1/2 MS, and seedlings at 2 dpg were transferred to 1/2 MS or 50 mM medium for 4 days. Seedings with NaCl treatment were transferred back to 1/2 MS medium for recovery for 4 days before imaging. Black lines represent position of primary root tips. Scale bars, 1 cm.

## SUPPLEMENTAL INFORMATION

Supplemental information can be found online at https://doi.org/10.1016/j.devcel.2023.06.012.

## ACKNOWLEDGMENTS

We thank Philip Benfey, Zhizhong Gong, and Chuanyou Li for sharing research materials. We thank Huicong Zhang for the help of data analysis. We greatly appreciated helpful discussions with all members from the Guo lab. This work was supported by National Natural Science Foundation of China (32130007 and 31921001) (Y.G.) and National Natural Science Foundation of China (32070874 and 32270299) (W.Z.).

## AUTHOR CONTRIBUTIONS

R.H., W.Z., and Y.G. designed the experiments. R.H. carried out most of the experiments and prepared the figures. M.L. performed some of the *in vitro* kinase experiments. J.L. performed the root tip RNA-seq experiment. R.H., W.Z., M.L., J.L., B.S., and Y.G. analyzed the data. B.S. provided materials for the study. R.H., W.Z., B.S., and Y.G. wrote the manuscript.

## DECLARATION OF INTERESTS

The authors declare no competing interests.

Received: June 6, 2022
Revised: April 2, 2023
Accepted: June 30, 2023
Published: July 21, 2023

## REFERENCES

1. Van Zelm, E., Zhang, Y., and Testerink, C. (2020). Salt tolerance mechanisms of plants. Annu. Rev. Plant Biol. *71*, 403–433. https://doi.org/10.1146/annurev-arplant-050718-100005.
2. Yang, Y., and Guo, Y. (2018). Elucidating the molecular mechanisms mediating plant salt-stress responses. New Phytol. *217*, 523–539. https://doi.org/10.1111/nph.14920.
3. Zhao, C., Zhang, H., Song, C., Zhu, J.K., and Shabala, S. (2020). Mechanisms of plant responses and adaptation to soil salinity. Innovation (Camb) *1*, 100017. https://doi.org/10.1016/j.xinn.2020.100017.
4. Ismail, A., Takeda, S., and Nick, P. (2014). Life and death under salt stress: same players, different timing? J. Exp. Bot. *65*, 2963–2979. https://doi.org/10.1093/jxb/eru159.
5. West, G., Inzé, D., and Beemster, G.T. (2004). Cell cycle modulation in the response of the primary root of Arabidopsis to salt stress. Plant Physiol. *135*, 1050–1058. https://doi.org/10.1104/pp.104.040022.
6. Korver, R.A., van den Berg, T., Meyer, A.J., Galvan-Ampudia, C.S., Ten Tusscher, K.H.W.J., and Testerink, C. (2020). Halotropism requires phospholipase Dzeta1-mediated modulation of cellular polarity of auxin transport carriers. Plant Cell Environ. *43*, 143–158. https://doi.org/10.1111/pce.13646.
7. Sun, F., Zhang, W., Hu, H., Li, B., Wang, Y., Zhao, Y., Li, K., Liu, M., and Li, X. (2008). Salt modulates gravity signaling pathway to regulate growth direction of primary roots in Arabidopsis. Plant Physiol. *146*, 178–188. https://doi.org/10.1104/pp.107.109413.
8. Van den Berg, T., Korver, R.A., Testerink, C., and Ten Tusscher, K.H. (2016). Modeling halotropism: a key role for root tip architecture and reflux loop remodeling in redistributing auxin. Development *143*, 3350–3362. https://doi.org/10.1242/dev.135111.
9. Wang, Y., Li, K., and Li, X. (2009). Auxin redistribution modulates plastic development of root system architecture under salt stress in *Arabidopsis thaliana*. J. Plant Physiol. *166*, 1637–1645. https://doi.org/10.1016/j.jplph.2009.04.009.
10. Halfter, U., Ishitani, M., and Zhu, J.K. (2000). The Arabidopsis SOS2 protein kinase physically interacts with and is activated by the calcium-binding protein SOS3. Proc. Natl. Acad. Sci. USA *97*, 3735–3740. https://doi.org/10.1073/pnas.97.7.3735.
11. Lin, H., Yang, Y., Quan, R., Mendoza, I., Wu, Y., Du, W., Zhao, S., Schumaker, K.S., Pardo, J.M., and Guo, Y. (2009). Phosphorylation of SOS3-LIKE CALCIUM BINDING PROTEIN8 by SOS2 protein kinase stabilizes their protein complex and regulates salt tolerance in Arabidopsis. Plant Cell *21*, 1607–1619. https://doi.org/10.1105/tpc.109.066217.
12. Liu, J., Ishitani, M., Halfter, U., Kim, C.S., and Zhu, J.K. (2000). The Arabidopsis thaliana SOS2 gene encodes a protein kinase that is required for salt tolerance. Proc. Natl. Acad. Sci. USA *97*, 3730–3734. https://doi.org/10.1073/pnas.97.7.3730.
13. Ma, L., Ye, J., Yang, Y., Lin, H., Yue, L., Luo, J., Long, Y., Fu, H., Liu, X., Zhang, Y., et al. (2019). The SOS2-SCaBP8 complex generates and fine-tunes an AtANN4-dependent calcium signature under salt stress. Dev. Cell *48*, 697–709.e5. https://doi.org/10.1016/j.devcel.2019.02.010.
14. Shi, H., Ishitani, M., Kim, C., and Zhu, J.K. (2000). The Arabidopsis thaliana salt tolerance gene SOS1 encodes a putative $Na^+/H^+$ antiporter. Proc. Natl. Acad. Sci. USA *97*, 6896–6901. https://doi.org/10.1073/pnas.120170197.
15. Zhu, J.K. (2002). Salt and drought stress signal transduction in plants. Annu. Rev. Plant Biol. *53*, 247–273. https://doi.org/10.1146/annurev.arplant.53.091401.143329.
16. Knight, H., Trewavas, A.J., and Knight, M.R. (1997). Calcium signalling in Arabidopsis thaliana responding to drought and salinity. Plant J. *12*, 1067–1078. https://doi.org/10.1046/j.1365-313x.1997.12051067.x.
17. Ishitani, M., Liu, J., Halfter, U., Kim, C.S., Shi, W., and Zhu, J.K. (2000). SOS3 function in plant salt tolerance requires N-myristoylation and calcium binding. Plant Cell *12*, 1667–1678. https://doi.org/10.1105/tpc.12.9.1667.
18. Liu, J., and Zhu, J.K. (1998). A calcium sensor homolog required for plant salt tolerance. Science *280*, 1943–1945. https://doi.org/10.1126/science.280.5371.1943.
19. Quan, R., Lin, H., Mendoza, I., Zhang, Y., Cao, W., Yang, Y., Shang, M., Chen, S., Pardo, J.M., and Guo, Y. (2007). SCABP8/CBL10, a putative calcium sensor, interacts with the protein kinase SOS2 to protect Arabidopsis shoots from salt stress. Plant Cell *19*, 1415–1431. https://doi.org/10.1105/tpc.106.042291.
20. Zhao, Y.K., Wang, T., Zhang, W.S., and Li, X. (2011). SOS3 mediates lateral root development under low salt stress through regulation of auxin redistribution and maxima in Arabidopsis. New Phytol. *189*, 1122–1134. https://doi.org/10.1111/j.1469-8137.2010.03545.x.
21. Scheres, B., Benfey, P., and Dolan, L. (2002). Root development. Arabidopsis Book *1*, e0101. https://doi.org/10.1199/tab.0101.
22. Zhou, W.K., Wei, L.R., Xu, J.A., Zhai, Q.Z., Jiang, H.L., Chen, R., Chen, Q.A., Sun, J.Q., Chu, J.F., Zhu, L.H., et al. (2010). Arabidopsis tyrosylprotein sulfotransferase acts in the Auxin/PLETHORA pathway in regulating postembryonic maintenance of the root stem cell niche. Plant Cell *22*, 3692–3709. https://doi.org/10.1105/tpc.110.075721.
23. Cui, H., Levesque, M.P., Vernoux, T., Jung, J.W., Paquette, A.J., Gallagher, K.L., Wang, J.Y., Blilou, I., Scheres, B., and Benfey, P.N. (2007). An evolutionarily conserved mechanism delimiting SHR movement defines a single layer of endodermis in plants. Science *316*, 421–425. https://doi.org/10.1126/science.1139531.
24. Di Laurenzio, L., Wysocka-Diller, J., Malamy, J.E., Pysh, L., Helariutta, Y., Freshour, G., Hahn, M.G., Feldmann, K.A., and Benfey, P.N. (1996). The SCARECROW gene regulates an asymmetric cell division that is essential for generating the radial organization of the Arabidopsis root. Cell *86*, 423–433. https://doi.org/10.1016/s0092-8674(00)80115-4.
25. Helariutta, Y., Fukaki, H., Wysocka-Diller, J., Nakajima, K., Jung, J., Sena, G., Hauser, M.T., and Benfey, P.N. (2000). The SHORT-ROOT gene controls radial patterning of the Arabidopsis root through radial signaling. Cell *101*, 555–567. https://doi.org/10.1016/s0092-8674(00)80865-x.
26. Shimotohno, A., Heidstra, R., Blilou, I., and Scheres, B. (2018). Root stem cell niche organizer specification by molecular convergence of

PLETHORA and SCARECROW transcription factor modules. Genes Dev. *32*, 1085–1100. https://doi.org/10.1101/gad.314096.118.

27. Sozzani, R., Cui, H., Moreno-Risueno, M.A., Busch, W., Van Norman, J.M., Vernoux, T., Brady, S.M., Dewitte, W., Murray, J.A., and Benfey, P.N. (2010). Spatiotemporal regulation of cell-cycle genes by SHORTROOT links patterning and growth. Nature *466*, 128–132. https://doi.org/10.1038/nature09143.
28. Zhai, H.W., Zhang, X.Y., You, Y.R., Lin, L.H., Zhou, W.K., and Li, C.Y. (2020). SEUSS integrates transcriptional and epigenetic control of root stem cell organizer specification. EMBO J. *39*, e105047. https://doi.org/10.15252/embj.2020105047.
29. Zhang, X.Y., Zhou, W.K., Chen, Q., Fang, M.M., Zheng, S.S., Scheres, B., and Li, C.Y. (2018). Mediator subunit MED31 is required for radial patterning of Arabidopsis roots. Proc. Natl. Acad. Sci. USA *115*, E5624–E5633. https://doi.org/10.1073/pnas.1800592115.
30. Aida, M., Beis, D., Heidstra, R., Willemsen, V., Blilou, I., Galinha, C., Nussaume, L., Noh, Y.S., Amasino, R., and Scheres, B. (2004). The PLETHORA genes mediate patterning of the Arabidopsis root stem cell niche. Cell *119*, 109–120. https://doi.org/10.1016/j.cell.2004.09.018.
31. Galinha, C., Hofhuis, H., Luijten, M., Willemsen, V., Blilou, I., Heidstra, R., and Scheres, B. (2007). PLETHORA proteins as dose-dependent master regulators of *Arabidopsis* root development. Nature *449*, 1053–1057. https://doi.org/10.1038/nature06206.
32. Mähönen, A.P., ten Tusscher, K., Siligato, R., Smetana, O., Díaz-Triviño, S., Salojärvi, J., Wachsman, G., Prasad, K., Heidstra, R., and Scheres, B. (2014). PLETHORA gradient formation mechanism separates auxin responses. Nature *515*, 125–129. https://doi.org/10.1038/nature13663.
33. Blilou, I., Xu, J., Wildwater, M., Willemsen, V., Paponov, I., Friml, J., Heidstra, R., Aida, M., Palme, K., and Scheres, B. (2005). The PIN auxin efflux facilitator network controls growth and patterning in Arabidopsis roots. Nature *433*, 39–44. https://doi.org/10.1038/nature03184.
34. Matsuzaki, Y., Ogawa-Ohnishi, M., Mori, A., and Matsubayashi, Y. (2010). Secreted peptide signals required for maintenance of root stem cell niche in *Arabidopsis*. Science *329*, 1065–1067. https://doi.org/10.1126/science.1191132.
35. Ou, Y., Lu, X.T., Zi, Q.N., Xun, Q.Q., Zhang, J.J., Wu, Y.J., Shi, H.Y., Wei, Z.Y., Zhao, B.L., Zhang, X.Y., et al. (2016). RGF1 INSENSITIVE 1 to 5, a group of LRR receptor-like kinases, are essential for the perception of root meristem growth factor 1 in *Arabidopsis thaliana*. Cell Res. *26*, 686–698. https://doi.org/10.1038/cr.2016.63.
36. Shinohara, H., Mori, A., Yasue, N., Sumida, K., and Matsubayashi, Y. (2016). Identification of three LRR-RKs involved in perception of root meristem growth factor in Arabidopsis. Proc. Natl. Acad. Sci. USA *113*, 3897–3902. https://doi.org/10.1073/pnas.1522639113.
37. Yamada, M., Han, X.W., and Benfey, P.N. (2020). RGF1 controls root meristem size through ROS signalling. Nature *577*, 85–88. https://doi.org/10.1038/s41586-019-1819-6.
38. Dinneny, J.R., Long, T.A., Wang, J.Y., Jung, J.W., Mace, D., Pointer, S., Barron, C., Brady, S.M., Schiefelbein, J., and Benfey, P.N. (2008). Cell identity mediates the response of Arabidopsis roots to abiotic stress. Science *320*, 942–945. https://doi.org/10.1126/science.1153795.
39. Zhang, H., Guo, L., Li, Y.P., Zhao, D., Liu, L.P., Chang, W.W., Zhang, K., Zheng, Y.C., Hou, J.J., Fu, C.H., et al. (2022). TOP1α fine-tunes TOR-PLT2 to maintain root tip homeostasis in response to sugars. Nat. Plants *8*, 792–801. https://doi.org/10.1038/s41477-022-01179-x.
40. Holsters, M., Silva, B., Van Vliet, F., Genetello, C., De Block, M., Dhaese, P., Depicker, A., Inzé, D., Engler, G., and Villarroel, R. (1980). The functional organization of the nopaline A. tumefaciens plasmid pTiC58. Plasmid *3*, 212–230. https://doi.org/10.1016/0147-619x(80)90110-9.
41. Fukaki, H., Wysocka-Diller, J., Kato, T., Fujisawa, H., Benfey, P.N., and Tasaka, M. (1998). Genetic evidence that the endodermis is essential for shoot gravitropism in *Arabidopsis thaliana*. Plant J. *14*, 425–430. https://doi.org/10.1046/j.1365-313x.1998.00137.x.
42. Kornet, N., and Scheres, B. (2009). Members of the GCN5 histone acetyltransferase complex regulate PLETHORA-mediated root stem cell niche maintenance and transit amplifying cell proliferation in Arabidopsis. Plant Cell *21*, 1070–1079. https://doi.org/10.1105/tpc.108.065300.
43. Brownfield, L., Hafidh, S., Borg, M., Sidorova, A., Mori, T., and Twell, D. (2009). A plant germline-specific integrator of sperm specification and cell cycle progression. PLoS Genet. *5*, e1000430. https://doi.org/10.1371/journal.pgen.1000430.
44. Li, J., Zhou, H., Zhang, Y., Li, Z., Yang, Y., and Guo, Y. (2020). The GSK3-like kinase BIN2 is a molecular switch between the salt stress response and growth recovery in *Arabidopsis thaliana*. Dev. Cell *55*, 367–380.e6. https://doi.org/10.1016/j.devcel.2020.08.005.
45. Zhu, J.K., Liu, J., and Xiong, L. (1998). Genetic analysis of salt tolerance in Arabidopsis. Evidence for a critical role of potassium nutrition. Plant Cell *10*, 1181–1191. https://doi.org/10.1105/tpc.10.7.1181.
46. Zhou, W.K., Lozano-Torres, J.L., Blilou, I., Zhang, X.Y., Zhai, Q.Z., Smant, G., Li, C.Y., and Scheres, B. (2019). A jasmonate signaling network activates root stem cells and promotes regeneration. Cell *177*, 942–956.e14. https://doi.org/10.1016/j.cell.2019.03.006.
47. Horvath, B.M., Kourova, H., Nagy, S., Nemeth, E., Magyar, Z., Papdi, C., Ahmad, Z., Sanchez-Perez, G.F., Perilli, S., Blilou, I., et al. (2017). Arabidopsis RETINOBLASTOMA RELATED directly regulates DNA damage responses through functions beyond cell cycle control. EMBO J. *36*, 1261–1278. https://doi.org/10.15252/embj.201694561.
48. Chen, H., Zou, Y., Shang, Y., Lin, H., Wang, Y., Cai, R., Tang, X., and Zhou, J.M. (2008). Firefly luciferase complementation imaging assay for protein-protein interactions in plants. Plant Physiol. *146*, 368–376. https://doi.org/10.1104/pp.107.111740.
49. Waadt, R., Schmidt, L.K., Lohse, M., Hashimoto, K., Bock, R., and Kudla, J. (2008). Multicolor bimolecular fluorescence complementation reveals simultaneous formation of alternative CBL/CIPK complexes in planta. Plant J. *56*, 505–516. https://doi.org/10.1111/j.1365-313X.2008.03612.x.
50. Ma, L., Han, R., Yang, Y., Liu, X., Li, H., Zhao, X., Li, J., Fu, H., Huo, Y., Sun, L., et al. (2023). Phytochromes enhance SOS2-mediated PIF1 and PIF3 phosphorylation and degradation to promote *Arabidopsis* salt tolerance. Plant Cell. https://doi.org/10.1093/plcell/koad117.
51. Nie, K., Zhao, H., Wang, X., Niu, Y., Zhou, H., and Zheng, Y. (2022). The MIEL1-ABI5/MYB30 regulatory module fine tunes abscisic acid signaling during seed germination. J. Integr. Plant Biol. *64*, 930–941. https://doi.org/10.1111/jipb.13234.
52. Kong, L., Cheng, J., Zhu, Y., Ding, Y., Meng, J., Chen, Z., Xie, Q., Guo, Y., Li, J., Yang, S., et al. (2015). Degradation of the ABA co-receptor ABI1 by PUB12/13 U-box E3 ligases. Nat. Commun. *6*, 8630. https://doi.org/10.1038/ncomms9630.
53. Wang, F., Zhu, D., Huang, X., Li, S., Gong, Y., Yao, Q., Fu, X., Fan, L.M., and Deng, X.W. (2009). Biochemical insights on degradation of Arabidopsis della proteins gained from a cell-free assay system. Plant Cell *21*, 2378–2390. https://doi.org/10.1105/tpc.108.065433.
54. Bray, N.L., Pimentel, H., Melsted, P., and Pachter, L. (2016). Near-optimal probabilistic RNA-seq quantification. Nat. Biotechnol. *34*, 525–527. https://doi.org/10.1038/nbt.3519.
55. Pimentel, H., Bray, N.L., Puente, S., Melsted, P., and Pachter, L. (2017). Differential analysis of RNA-seq incorporating quantification uncertainty. Nat. Methods *14*, 687–690. https://doi.org/10.1038/nmeth.4324.

## STAR★METHODS

### KEY RESOURCES TABLE

| REAGENT or RESOURCE | SOURCE | IDENTIFIER |
|---|---|---|
| **Antibodies** | | |
| Rabbit polyclonal Anti-GFP | Easybio | Cat# 80790412; RRID: AB_2313773 |
| Mouse monoclonal Anti-MBP | NEB | Cat# E8032S; RRID: AB_2313773 |
| Mouse monoclonal Anti-actin | CWBIO | Cat# 01265; RRID: AB_2313773 |
| **Bacterial Strains** | | |
| *Agobacterium tumefaciens* GV3101 | Holsters et al.[40] | N/A |
| *Escherichia coli* BL21 | TransGen Biotech | Cat# CD901-03 |
| *Escherichia coli* DH5α | TransGen Biotech | Cat# CD201-01 |
| **Chemicals, Peptides** | | |
| Propidium Iodide (PI) | invitrogen | Cat# 1743734 |
| Amylose Resin | NEB | Cat# E8021S |
| Ni-NTA Agarose | MCLAB | Cat# NINTA-300 |
| D-Luciferin | BioVision | Cat# 306 |
| Phosphatase inhibitor cocktail | bimake | Cat# B15001 |
| Murashige Skoog | phytotechlab | Cat# M519 |
| Protease Inhibitor Cocktail Tablets | Roche | Cat# 04693116001 |
| MG132 | Sigma-Aldrich | Cat# C2211 |
| MG115 | APExBIO | Cat# A2612 |
| 3-MA (3-Methyladenine) | MedCheMExpress | Cat# 5142-23-4 |
| β-estradiol | Sigma-Aldrich | Cat# SLBL7310V |
| **Critical Commercial Assays** | | |
| TRIGene | GenStar | Cat# P118-05 |
| ClonExpress Ultra One Step Cloning Kit | Vazyme | Cat# C115-01 |
| Mut Express II Fast Mutagenesis Kit V2 | Vazyme | Cat# C214-01 |
| PrimeScript™ RT reagent kit | TaKaRa | Cat# RR047A |
| TB Green™ Premix Ex Taq™ | TaKaRa | Cat# RR420A |
| Cell Proliferation EdU Image Kit (orange Fluorescence) | Abbkine | Cat# KTA2031-EN |
| TRIzol™ Reagent | Invitrogen | Cat# 15596026 |
| VAHTS RNA-seq Library Prep Kit | Vayme | Cat# NR605 |
| **Deposited Data** | | |
| The Arabidopsis thaliana genome (TAIR10) | The Arabidopsis Information Resource | www.arabidopsis.org |
| Raw and analyzed RNA sequencing data for WT and sos2-2 with salt treatment | This paper | GEO: GSE228893 |
| Original data | This papar | https://doi.org/10.17632/pvjwcthdhn.1 |
| **Experimental Models: Organisms/Strains** | | |
| *Arabidopsis*: Wild-type (Col) | N/A | N/A |
| *Arabidopsis*: *gl1* | Quan et al.[19] | N/A |
| *Arabidopsis*: *sos2-2* | Quan et al.[19] | N/A |
| *Arabidopsis*: *plt1-4* | Aida et al.[30] | N/A |
| *Arabidopsis*: *plt2-2* | Aida et al.[30] | N/A |
| *Arabidopsis*: *plt1-4 plt2-2* | Aida et al.[30] | N/A |
| *Arabidopsis*: *shr-2* | Helariutta et al.[25] | N/A |
| *Arabidopsis*: *scr-3* | Fukaki et al.[41] | N/A |
| *Arabidopsis*: *pPLT1:PLT1-YFP* | Kornet and Scheres[42] | N/A |

(*Continued on next page*)

*Continued*

| REAGENT or RESOURCE | SOURCE | IDENTIFIER |
|---|---|---|
| *Arabidopsis*: *pPLT1:PLT1-YFP sos2-2* | This paper | N/A |
| *Arabidopsis*: *pPLT2:PLT2-YFP* | Kornet and Scheres[42] | N/A |
| *Arabidopsis*: *pPLT2:PLT2-YFP sos2-2* | This paper | N/A |
| *Arabidopsis*: *pPLT1:CFP* | Kornet and Scheres[42] | N/A |
| *Arabidopsis*: *pPLT1:CFP sos2-2* | This paper | N/A |
| *Arabidopsis: pPLT2:CFP* | Kornet and Scheres[42] | N/A |
| *Arabidopsis: pPLT2:CFP sos2-2* | This paper | N/A |
| *Arabidopsis: pCYCB1;1:GFP* | Brownfield et al.[43] | N/A |
| *Arabidopsis: pCYCB1;1:GFP sos2-2* | This paper | N/A |
| *Arabidopsis: pPLT2:GFP-PLT2$^{S3E}$ sos2-2* | This paper | N/A |
| *Arabidopsis: pPLT2:GFP-PLT2$^{S3A}$ sos2-2* | This paper | N/A |
| *Arabidopsis: pPLT1:GFP-PLT1$^{S4D}$ sos2-2* | This paper | N/A |
| *Arabidopsis: pPLT1:GFP-PLT1$^{S4A}$ sos2-2* | This paper | N/A |
| *Arabidopsis: pPLT1:GFP-PLT1$^{S4D}$ pPLT2:GFP-PLT2$^{S3E}$ sos2-2* | This paper | N/A |
| *Arabidopsis: pPLT2:GFP-PLT2 plt1-4 plt2-2* | This paper | N/A |
| *Arabidopsis: pPLT2:GFP-PLT2$^{S3E}$ plt1-4 plt2-2* | This paper | N/A |
| *Arabidopsis: pPLT2:GFP-PLT2$^{S3A}$ plt1-4 plt2-2* | This paper | N/A |
| *Arabidopsis: pPLT1:GFP-PLT1$^{S4D}$ plt1-4 plt2-2* | This paper | N/A |
| *Arabidopsis: pPLT1:GFP-PLT1$^{S4A}$ plt1-4 plt2-2* | This paper | N/A |
| Oligonucleotides | | |
| Primers used in this study, see Table S1 | | |
| Recombinant DNA | | |
| pET28a-SOS2 | Li et al.[44] | N/A |
| pMAL-c5x-PLT1 | This paper | N/A |
| pMAL-c5x-PLT2 | This paper | N/A |
| pMAL-c5x-PLT1 1-178 AA | This paper | N/A |
| pMAL-c5x-PLT1 179-380 AA | This paper | N/A |
| pMAL-c5x-PLT1 381-574 AA | This paper | N/A |
| pMAL-c5x-PLT2 1-187 AA | This paper | N/A |
| pMAL-c5x-PLT2 188-388 AA | This paper | N/A |
| pMAL-c5x-PLT2 389-568 AA | This paper | N/A |
| pMAL-c5x-PLT1$^{S4A}$ | This paper | N/A |
| pMAL-c5x-PLT1$^{S4D}$ | This paper | N/A |
| pMAL-c5x-PLT2$^{S3A}$ | This paper | N/A |
| pMAL-c5x-PLT2$^{S3E}$ | This paper | N/A |
| pSPYCE-SOS2 | Li et al.[44] | N/A |
| pSPYNE-GUS | Li et al.[44] | N/A |
| pSPYCE (MR)-GUS | Li et al.[44] | N/A |
| pSPYNE-PLT1 | This paper | N/A |
| pSPYNE-PLT2 | This paper | N/A |
| pCambia1300-SOS2-nLUC | Li et al.[44] | N/A |
| pCambia1300-GUS-nLUC | Li et al.[44] | N/A |
| pCambia1300-cLUC-GUS | Li et al.[44] | N/A |
| pCambia1300-cLUC-PLT1 | This paper | N/A |
| pCambia1300-cLUC-PLT1$^{S4A}$ | This paper | N/A |
| pCambia1300-cLUC-PLT1$^{S4D}$ | This paper | N/A |
| pCambia1300-cLUC-PLT2$^{S3A}$ | This paper | N/A |
| pCambia1300-cLUC-PLT2$^{S3E}$ | This paper | N/A |
| pCambia1300-pPLT2:GFP-PLT2 | This paper | N/A |

(*Continued on next page*)

| Continued | | |
|---|---|---|
| REAGENT or RESOURCE | SOURCE | IDENTIFIER |
| pCambia1300-pPLT2:GFP-PLT2$^{S3E}$ | This paper | N/A |
| pCambia1300-pPLT2:GFP-PLT2$^{S3A}$ | This paper | N/A |
| pCambia1300-pPLT1:GFP-PLT1 | This paper | N/A |
| pCambia1300-pPLT1:GFP-PLT1$^{S4D}$ | This paper | N/A |
| pCambia1300-pPLT1:GFP-PLT1$^{S4A}$ | This paper | N/A |
| Software | | |
| ImageJ | https://imagej.nih.gov/ij/ | |
| GraphPad Prism 7.00 | http://graphpad-prism.software.informer.com/7.00/ | |
| R software | https://www.r-project.org | |
| BioRender | https://www.biorender.com/ | |

## RESOURCE AVAILABILITY

### Lead contact

Further information and requests for resources and reagents should be directed to and will be fulfilled by the lead contact, Yan Guo (guoyan@cau.edu.cn).

### Materials availability

This study did not generate new unique reagents. The plasmids generated in this study will be made available upon request.

### Data and code availability

RNA sequencing data in this paper have been deposited at GEO: GSE228893. Original data have been deposited to Mendeley Data: https://doi.org/10.17632/pvjwcthdhn.1. Any additional information required to reanalyze the data reported in this work paper is available from the lead contact upon request.

## EXPERIMENTAL MODEL AND STUDY PARTICIPANT DETAILS

### Plants materials and growth conditions

*Arabidopsis thaliana* ecotype Col-0 and Ws were used as wild-type control. Mutants used in this study: *plt1-4* (Ws), *plt2-2* (Ws), *plt1-4 plt2-2* (Ws), *shr-2* (Col-0), *scr-3* (Col-0), *gl1* (Col-0). The *sos2-2* mutant (but see Liu et al.[12] and Zhu et al.[45]) was in the *gl1* mutant background, and *GL1* mutation did not affect its salt sensitivity compared with Col-0 (but see Quan et al.[19]). Seeds were sterilized and plated on 1/2 Murashige and Skoog (MS) medium or 1/2 MS medium containing 25 mM/50 mM/100 mM NaCl with 1% sucrose and 0.8% agar. Plates were stratified at 4°C for 3 days, and then were placed in a growth chamber at 22°C with a 16 h light/8 h dark photoperiod with illumination 120 μmol $m^{-2}$ $s^{-1}$.

## METHOD DETAILS

### Plasmid construction and plant transformation

*pPLT1::GFP* and *pPLT2::GFP* was constructed by fusing a 4500 bp *PLT1* and 5800 bp *PLT2* promoter fragment in front of green fluorescence protein (GFP) in the *pCAMBIA-1300* vector, respectively. And the full-length genomic *PLT1* and *PLT2* (original or mutated) were cloned into the *pPLT1::GFP* and *pPLT2::GFP* vectors respectively to generate *pPLT1::GFP-PLT1* (WT/S4A/S4D) and *pPLT2::GFP-PLT2* (WT/S3A/S3E) constructs. Constructs were transformed into strain *Agrobacterium tumefaciens* GV3101 and transformed into *Arabidopsis thaliana* by floral dip. Transformed plants were selected based on their resistance to hygromycin. Homozygous T3 or T4 transgenic plants were used for analysis.

### Salt treatment assay

For experiments in Figures 1 and S1, seeds were sown on 1/2 MS ± 50 mM NaCl, and analysed at indicated days post germination (dpg). For the rest experiment, seeds were sown on 1/2 MS medium, and then transferred to 1/2 MS plates ± indicated concentrations of NaCl. The camera and confocal images for phenotypic assays were taken at 1, 3 or 5 days after transfer, respectively. For *in vivo* protein extract assays, seedlings were treated with 1/2 MS liquid medium with 100 mM NaCl. To determine salt sensitivity in soil, 10-d-old seedlings of Col-0, indicated mutants and transgenic plants were grown in growth chambers under short-day conditions (12-h-light/12-h-dark photoperiod) for 2.5 weeks. Subsequently, the soil was irrigated with 50 mM NaCl or 0 mM water for four times. Plants were grown for an additional 1.5-2 weeks and were photographed.

### Microscopy

For confocal laser scanning microscopy, the root tips were stained in 20 μg/mL propidium iodide and observed using a Lecia sp8 system. PI was visualized using wavelengths of 600-640 nm. The CFP, GFP and YFP were used wavelengths of 450-480, 500-540 and 525-565 nm, respectively. Images were taken with LAS X software and processed with canvas. Modified pseudo-Schiff propidium iodide (mPS-PI) staining was performed as described previously by Zhou et al.[46] Samples were fixed (10% acetic acid, 50% methanol) and kept at 4°C for overnight, rinsed briefly with water, and incubated in 1% periodic acid (an oxidizing agent) for 40 minutes - 1 hour. After that, samples were washed with water and incubated in Schiff reagent with propidium iodide (100 mM sodium metabisulphite; 0.15 N HCl; 100 μg/mL PI) for 2 hours before imaging.

### EdU Staining

EdU Staining was performed as described previously by Horvath et al.[47] Seedlings at 2 dpg were incubated with 1/2 MS liquid medium with 10 μM EdU (Cell Proliferation EdU Image Kit (orange Fluorescence)) for 6 h. Seedlings were then fixed in freshly prepared fixative solution containing 3.7% (v/v) paraformaldehyde and 1% (v/v) Triton-X 100 in 1 × PBS solution for 1 h and washed twice with 3% (w/v) bovine serium albumin (BSA) in 1 × PBS solution. Seedlings were then incubated with 100 μl Click-iT reaction mix (Abbkine Click-iT Cell Proliferation EdU Image Kit (orange Fluorescence) KTA2031-EN; 76 μl of Deionized Water, 10 μl 10 × reaction buffer, 4 μl of Copper Reagent, 0.2 μl of AbFluor 545 azide and 10 μl of 10 × Reducing Agent) for 1 h protected from light at room temperature. The stained seedlings were then washed once with 3% (w/v) BSA in 1 × PBS solution and then stored in 1 × PBS solution protected from light until imaging. The labeled DNA in the sample was analyzed by fluorescence microscopy (Ex/Em=546/565 nm).

### Split-Luciferase assay (Split-LUC)

The coding sequences of *PLT1*, *PLT2*, *PLT1*$^{S4D}$, *PLT*$^{S4A}$, *PLT2*$^{S3E}$ and *PLT2*$^{S3A}$ were cloned into the *pCMABIA1300-cLUC* vector, respectively. The coding sequence of SOS2 was cloned into the *pCMABIA1300-nLUC* vector. The constructs were transformed into *Agrobacterium tumefaciens* GV3101. Agrobacteria were resuspended by medium (1/2 MS liquid medium add 200 μM Acetosyringone) and were infiltrated onto *Nicotiana benthamiana* leaves in pair for transient expression as described by Chen et al.[48] At 24-48 h after infiltration, the *Nicotiana benthamiana* leaves were applied with 1 mM D-luciferin in dark for 5 mins before detection. The LUC signal was detected by the cold charge-coupled device camera (Nikon-L936; Andor Tech). GUS-nLuc and cLuc-GUS were served as negative controls.

### Bimolecular fluorescence complementation (BIFC)

The coding sequences of PLT1 and PLT2 were cloned into the pSPYNE vector (but see Waadt et al.[49]), respectively. The coding sequence of SOS2 were cloned into the pSPYCE vector (but see Li et al.[44]). The BiFC experiments were performed as described by Waadt et al.[49] The pairwise constructs were infiltrated onto *Nicotiana benthamiana* leaves for transient expression. The YFP fluorescence signals were detected by the Zeiss 880 confocal laser scanning microscope. Images were taken with ZEN software and processed with canvas.

### Recombinant protein purification and *in vitro* kinase assay

All His- or MBP- fusion protein constructs were transformed into *Escherichia coli* BL21 (DE3) cells and recombinant proteins were induced by 0.5 mM isopropyl-β-thiogalactopyraniside (IPTG) at 16°C for over-night. The recombinant proteins were purified according to the manufacturer's protocol. *In vitro* kinase assay was conducted as described by Ma et al.[50] Every reaction containing the kinase His-SOS2 and the recombinant MBP-PLT1/2 (original, mutated or truncated) proteins in kinase buffer ( 20 mM Tirs-HCl, pH 8.0, 5 mM $MgCl_2$, 1 mM DTT, 10 μL [$^{31}$P] ATP) adding 0.1 μL [γ-$^{32}$ P] ATP (1 μCi) were incubated at 30°C for 30 min. The 6 × SDS loading buffer was incubated with samples at 100°C for 5 min. The samples were separated by 10 % SDS-PAGE and stained by Coomassie Brilliant Blue R 250, and then the gels were exposed to a phosphor screen (Amersham Biosciences). The phosphorylation signals were detected by a Typhoon 9410 phosphor imager (Amersham Biosciences).

### Immunoprecipitation assays

The immunoprecipitation assays were performed as described by Nie et al.[51] Seedlings at 6-7 dpg were treated with or without 100 mM NaCl liquid medium for indicated time. Seedlings were harvested and ground into fine powder in liquid nitrogen. Total proteins were extracted in IP buffer containing 50 mM Tris-HCl (pH 7.5), 150 mM NaCl, 10 mM $MgCl_2$, 10% (V/V) glycerine, 0.5% nonidet-P40, 5 mM DTT, 100 × protease inhibitor cocktail and 100 × phosphatase inhibitor cocktail. The protein abundance was detected by immunoblots using Anti-GFP, and β-ACTIN as a control.

### Cell-free

The cell-free assay was performed as described by Kong et al.[52] and Wang et al.[53] The 7-d-old of WT (*gl1*) or *sos2-2 Arabidopsis* seedlings were treated with or without 100 mM NaCl liquid medium for 24 h. Total proteins were subsequently extracted in degradation buffer containing 50 mM Tris-MES (pH=8.0), 0.5 M sucrose, 1 mM $MgCl_2$, 10 mM EDTA (pH=8.0), 4 mM, 5 mM DTT and 100 mM ATP. Cell debris were removed by 10 min centrifugation at 13000 g in 4°C twice. The 100 ng recombinant MBP-PLT1 (WT/S4A/S4D) or MBP-PLT2 (WT/S3A/S3D) proteins were incubated in 100 μL extracts (containing 500 μg total proteins) for the individual assays. The MG132, MG115 and 3MA were selectively added to extracts. The extracts were incubated at 22°C, samples

were detected by immunoblots using anti-MBP. The *β-ACTIN* was acted as loading control. The results were quantified using ImageJ software.

### Liquid Chromatography-Tandem Mass Spectrometry

To identify phosphorylation sites of PLT1 by SOS2 through liquid chromatography-tandem mass spectrometry (LC-MS/MS), 30 μg of His-SOS2 and 50 μg of MBP-PLT1 recombinant proteins were incubated in kinase buffer at 30°C for at least 30 min as described before by Ma et al.[50] The total sample was reduced by DTT, alkylated by IAM, digested by chymotrypsin overnight at 25°C, and subjected to LC-MS/MS.

### RNA-seq libraries Construction and High-Throughput Sequencing

Total RNA was extracted by using the TRIzol™ Reagent (Invitrogen) following the manual. Construction of RNA-seq libraries were performed using VAHTS RNA-seq Library Prep Kit (Vayme, NR605). Sequencing was performed on Illumina Novaseq platform. The tair10 Reference genome was downloaded from https://plants.ensembl.org/Arabidopsis_thaliana/Info/Index. The expression level of each transcript was estimated by using Kallisto_0.46.2. (but see Bray et al.[54]) Sleuth_0.30.0 was used for differential expression analysis (but see Pimentel et al.[55]). Differentially expressed genes were collected by using the following filters: fold-changed (FC) $\geqq$ 1.5 and p-value < 0.05. The heat map was drawn by R software (https://www.r-project.org).

### Total RNA Extraction for Quantitative RT-PCR

To analyse *PLT1, PLT2, CYCB1;1, CCS52A* and *CYCD3;3* at the transcriptional level, WT, *sos2-2*, and seedlings carrying the PLT1/2 phospho-mimetic and phospho-inactive variants at 5 dpg were treated with 50 mM NaCl treatment for indicated time and cut 1 cm from root tip. Total RNA was extracted with TRIGene reagent and reverse transcribed with PrimeScript™RT reagent kit with gDNA eraser. TB Green™Premix Ex Taq™ kit was used for the quantitative real-time PCR (qRT-PCR). qRT-PCR experiments were performed according to the instructions, and the relative gene expression abundance was calculated using ΔΔCt method. *ACTIN* was used as an internal control.

## QUANTIFICATION AND STATISTICAL ANALYSIS

For primary root, root meristem length and immunoblot were measured by ImageJ. The fluorescence intensity was measured on confocal images (LAX) software. Images were processed with Canvas. Statistical analysis of two groups was evaluated by Student's t test analysis. For multiple comparisons, one-way ANOVA or two-way ANOVA with post-hoc tests (Tukey's multiple comparisons test) were used. Data presented are mean values of at least three biological repeats with SD. Samples with different lowercase letters are statically different at $p < 0.001$, $< 0.01$ or $p < 0.05$.